Structure

Locally misfolded HER2 expressed on cancer cells is a promising target for development of cancer-specific antibodies

Graphical abstract

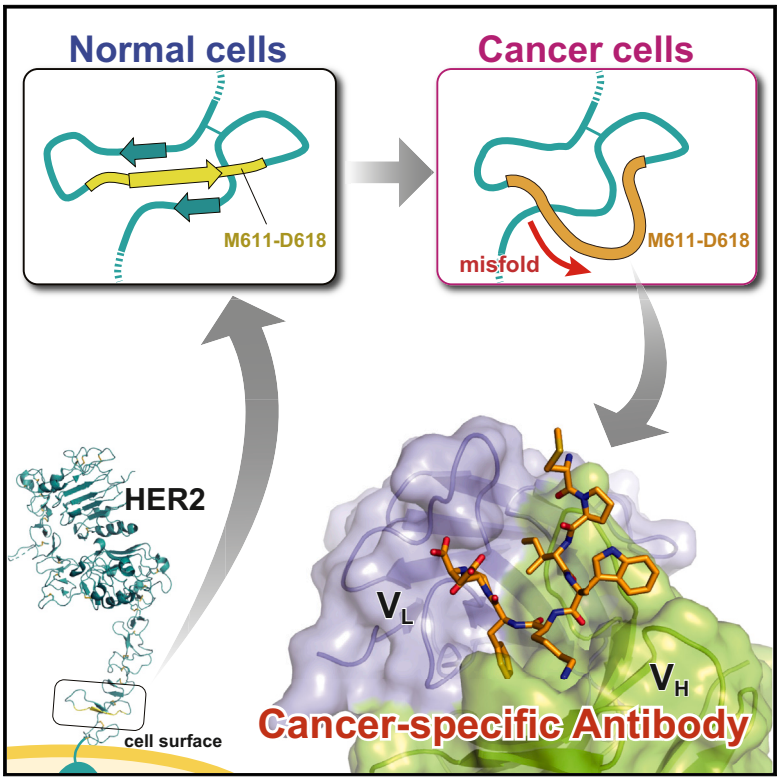

Authors

Takao Arimori, Emiko Mihara, Hiroyuki Suzuki, ..., Mika K. Kaneko, Junichi Takagi, Yukinari Kato

Correspondence

arimori@protein.osaka-u.ac.jp (T.A.), yukinari.kato.e6@tohoku.ac.jp (Y.K.)

In brief

Arimori et al. established a cancer-specific antibody that binds to human epidermal growth factor receptor 2 (HER2) on cancer cells but not to HER2 on normal cells. A crystal structure and cell-based binding analysis revealed that this specificity is due to the recognition of a local misfolded region, which is unique to HER2 on cancer cells.

Highlights

- A cancer-specific anti-HER2 antibody, H_2Mab-214, was established
- H_2Mab-214 binds only to HER2 on cancer cells, but not to HER2 on normal cells
- H_2Mab-214 recognizes a locally misfolded region of HER2
- Locally misfolded cell surface proteins can be targets for cancer-specific antibodies

Arimori et al., 2024, Structure *32*, 1–14
May 2, 2024
https://doi.org/10.1016/j.str.2024.02.007

CellPress

Structure

CellPress

Article

Locally misfolded HER2 expressed on cancer cells is a promising target for development of cancer-specific antibodies

Takao Arimori,[1,6,*] Emiko Mihara,[1] Hiroyuki Suzuki,[2,3] Tomokazu Ohishi,[4,5] Tomohiro Tanaka,[2] Mika K. Kaneko,[2,3] Junichi Takagi,[1] and Yukinari Kato[2,3,*]

[1]Institute for Protein Research, Osaka University, 3-2. Yamadaoka, Suita, Osaka 565-0871, Japan
[2]Department of Molecular Pharmacology, Tohoku University Graduate School of Medicine, 2-1, Seiryo-machi, Aoba-ku, Sendai, Miyagi 980-8575, Japan
[3]Department of Antibody Drug Development, Tohoku University Graduate School of Medicine, 2-1, Seiryo-machi, Aoba-ku, Sendai, Miyagi 980-8575, Japan
[4]Institute of Microbial Chemistry (BIKAKEN), Numazu, Microbial Chemistry Research Foundation, 18-24, Miyamoto, Numazu, Shizuoka 410-0301, Japan
[5]Institute of Microbial Chemistry (BIKAKEN), Laboratory of Oncology, Microbial Chemistry Research Foundation, 3-14-23, Kamiosaki, Shinagawa-ku, Tokyo 141-0021, Japan
[6]Lead contact
*Correspondence: arimori@protein.osaka-u.ac.jp (T.A.), yukinari.kato.e6@tohoku.ac.jp (Y.K.)
https://doi.org/10.1016/j.str.2024.02.007

SUMMARY

Overexpression of human epidermal growth factor receptor 2 (HER2) in breast and gastric cancers is associated with a poor prognosis, making it an important therapeutic target. Here, we establish a novel cancer-specific anti-HER2 antibody, H_2Mab-214. H_2Mab-214 reacts with HER2 on cancer cells, but unlike the therapeutic antibody trastuzumab, it does not react with HER2 on normal cells in flow cytometry measurements. A crystal structure suggests that H_2Mab-214 recognizes a structurally disrupted region in the HER2 domain IV, which normally forms a β-sheet. We show that this misfolding is inducible by site-directed mutagenesis mimicking the disulfide bond defects that also may occur in cancer cells, indicating that the local misfolding in the Cys-rich domain IV governs the cancer-specificity of H_2Mab-214. Furthermore, we show that H_2Mab-214 effectively suppresses tumor growth in xenograft mouse models. Our findings offer a potential strategy for developing cancer-specific therapeutic antibodies that target partially misfolded cell surface receptors.

INTRODUCTION

Human epidermal growth factor receptor (HER) family of receptor tyrosine kinases consists of four members: EGFR (HER1), HER2, HER3, and HER4. They play important roles in regulating cell proliferation, differentiation, and migration, while being implicated in many cancers. More than ten ligands for HER members have been identified, including epidermal growth factor, transforming growth factor α, and neuregulins (NRGs) 1–4, yet HER2 has no known direct activating ligand.[1] The extracellular region of all HER family members is commonly composed of four domains (I–IV). In the absence of ligands, those receptors other than HER2 are stabilized in an inactive "tethered" conformation where a protruding loop (also called dimerization arm) in the domain II interacts with the domain IV.[2–4] Upon ligand binding, the receptors undergo a large conformational change from "tethered" to "extended" and form homo- or heterodimers via the dimerization arm, resulting in the autophosphorylation of the cytoplasmic tyrosine kinase domain.[5–7] HER2 is unique in that it always adopts the extended conformation even in the monomeric state.[8] It has recently been shown that the structure of HER2 forming a heterodimer with HER3 is very similar to that of the monomeric state.[9] Hence, HER2 is always ready to be dimerized at cell surface, making it a preferable dimerization partner for other HER family members.[10] In addition, overexpression of HER2 promotes the formation of HER2 homodimers, leading to ligand-independent signaling.[11] HER2 overexpression is found in ~20% of breast cancers and is associated with poor prognosis, higher rates of recurrence, and shorter overall survival.[12] HER2 overexpression is also observed in a variety of other cancers, including gastric, bladder, ovarian, and non-small cell lung cancers.[13–16]

Trastuzumab, a monoclonal antibody (mAb) against HER2, recognizes the domain IV[8] and exhibits an anti-proliferating effect *in vitro* and a potent antitumor effect *in vivo*.[17] The addition of trastuzumab treatment to a standard chemotherapy improves objective response rates, progression-free survival, and overall survival in HER2-positive breast cancer patients with metastasis.[18] Trastuzumab has been the standard treatment for HER2-positive breast cancers[19] and HER2-positive gastric

Please cite this article in press as: Arimori et al., Locally misfolded HER2 expressed on cancer cells is a promising target for development of cancer-specific antibodies, Structure (2024), https://doi.org/10.1016/j.str.2024.02.007

cancers.[20] Clinically, the efficacy of trastuzumab involves immunologic engagement.[17] The Fc domain of trastuzumab mediates the engagement with Fcγ receptors (FcγRs) on various immune cells. Trastuzumab-FcγR binding allows for phagocytosis of antibody-bound tumor cells, which is called antibody-dependent cellular phagocytosis. The FcγR engagement also activates macrophages, dendritic cells, and neutrophils, which can change adaptive immune responses through chemotaxis, cytokine production, and antigen presentation. Furthermore, the FcγR engagement mediates the activation of natural killer (NK) cells which attack and lyse the target tumor cells, termed antibody-dependent cellular cytotoxicity (ADCC).[21] Margetuximab was developed by introducing several mutations in trastuzumab to improve the FcγRIIIA engagement (and thus ADCC activity),[22] and was approved by US Food and Drug Administration (FDA) and showed significant improvement in progression-free survival in heavily pretreated patients.[23,24] In addition to ADCC, trastuzumab is known to affect HER2 downstream signaling. Many *in vitro* experiments suggested that trastuzumab arrests the cell cycle through inhibiting the phosphatidylinositol 3-kinase (PI3K)/protein kinase B (AKT) signaling pathway, which is highly activated in a variety of cancers.[25] The detailed mechanism remains controversial, but this is recognized as one of the major mechanisms of action of trastuzumab, as is its ADCC activity.

Although trastuzumab exhibits potent antitumor effect, some patients develop resistance against trastuzumab treatment, which can be attributed to the hyperactivation caused by the heterodimerization with HER3.[26] Pertuzumab, another clinically approved HER2-targeting mAb, recognizes the domain II and prevents NRG1-induced heterodimerization with HER3 and intracellular signaling.[27] Thus, pertuzumab is considered to have a complementary mechanism of trastuzumab,[28] and the double anti-HER2 blockade has become the standard therapy in the initial management of metastatic HER2-positive breast cancer.[18] Furthermore, combination therapy using trastuzumab, pertuzumab, and chemotherapy has been evaluated and found to show even higher clinical benefit.[29]

Despite the proven success of HER2-targeted immunotherapies described previously, several adverse effects have also been reported, including cardiotoxicity.[30] Although they are not considered a clinically significant problem, routine cardiac monitoring is required in clinic during the anti-HER2 antibody treatment.[30] Interestingly, mice lacking *ErbB2* (ortholog of HER2) display embryonic lethality due to the dysfunctions associated with a lack of cardiac trabeculae,[31] and ventricular-restricted *ErbB2* deficiency in mice shows features of dilated cardiomyopathy.[32] These results indicate that HER2 plays important role(s) in normal heart development and homeostasis. As a proteomic study of healthy human tissues revealed a high level of broad expression of HER2,[33] anti-HER2 mAb therapies may attack normal tissues not limited to the heart, which could lead to other side effects including ones that are not clearly recognized at present. Therefore, it is highly desirable to use anti-HER2 mAbs that can exclusively recognize HER2 expressed on cancer cells, although such reagents have not been available to this day.

In this study, we succeeded in establishing a novel mAb that preferentially binds to HER2 expressed on cancer cells but not to HER2 expressed on normal cells. This antibody, H_2Mab-214, was established through standard immunization and hybridoma technology, but incorporating a special screening strategy called cancer-specific mAb or CasMab method we have developed previously.[34–37] The cancer-specificity of H_2Mab-214 was broadly investigated by flow cytometry analysis using various cell lines of normal or cancer origins, and its antitumor potential was confirmed by *in vivo* xenograft model. Most importantly, we clarified the molecular basis of H_2Mab-214's cancer selectivity by determining the crystal structure of its complex with HER2-derived peptide. Combined with the structure-guided mutagenesis at the epitope region, we show evidence that the local misfolding of HER2 domain IV Cys-rich region governs the cancer-specificity of H_2Mab-214, pointing toward a new way of searching cancer-specific antibodies against various cell surface receptors.

RESULTS

Cancer-specific HER2 recognition by H_2Mab-214

We have previously established a mouse anti-HER2 mAb H_2Mab-119 (IgG_1, kappa) by immunizing mice with HER2 ectodomain (HER2ec) produced in glioblastoma LN229 cells.[38] This antibody is judged as a pan-HER2 mAb that reacts with HER2 regardless of the cell type, because its FACS staining pattern is indistinguishable from that of trastuzumab (Figures 1A and 1B). In flow cytometric analysis using saturating concentrations of each antibody, H_2Mab-119 and trastuzumab brightly stained CHO-K1 cells expressing exogenously introduced HER2 (CHO/HER2) (Figure 1A) as well as BT-474 and SK-BR-3 breast cancer cell lines that are known to express endogenous HER2 (Figure 1B).[39] They also recognized immortalized normal cell lines, including HEK293T (embryonic kidney), HaCaT (keratinocyte), and MCF 10A (mammary gland epithelial cell), but not triple-negative breast cancer (TNBC) cell line, MDA-MB-468 cells known to be HER2-negative (Figure 1B).[40]

Next we aimed at obtaining anti-HER2 mAbs that recognize HER2 only when expressed on cancer cells. We incorporated differential screening protocol in the hybridoma selection step[34] and succeeded in establishing a few mAbs that recognized HER2-positive cancer cell lines, but not HER2-expressing normal cells. As shown in Figure 1B, one of the clones, H_2Mab-214 (mouse IgG_1, kappa), reacted with BT-474 and SK-BR-3 cells, but not with HEK293T, HaCaT, and MCF 10A cells. To eliminate the possibility that the differences in binding behavior between H_2Mab-214 and other two antibodies on flow cytometric analysis were due to differences in their affinity for HER2, ELISA-based affinity measurement was performed for these antibodies. The results showed that the K_D values of trastuzumab, H_2Mab-119, and H_2Mab-214 for recombinant soluble HER2ec were 0.31 nM, 0.30 nM, and 0.53 nM, respectively (Figure 1C), with the value of trastuzumab was comparable to that previously determined by a similar method.[41] As the K_D value of H_2Mab-214 was not significantly different from those of the other two antibodies, their binding behavior was shown to be affinity-independent. Binding of H_2Mab-214 was also observed with CHO cells overexpressing HER2 (Figure 1A), suggesting that the forced high-level expression in this normal cell line may render HER2 a H_2Mab-214 positive, cancer-like trait to some extent. Taken together, these results suggest that H_2Mab-214 exhibits specificity to HER2-positive breast cancer cells.

Please cite this article in press as: Arimori et al., Locally misfolded HER2 expressed on cancer cells is a promising target for development of cancer-specific antibodies, Structure (2024), https://doi.org/10.1016/j.str.2024.02.007

CellPress

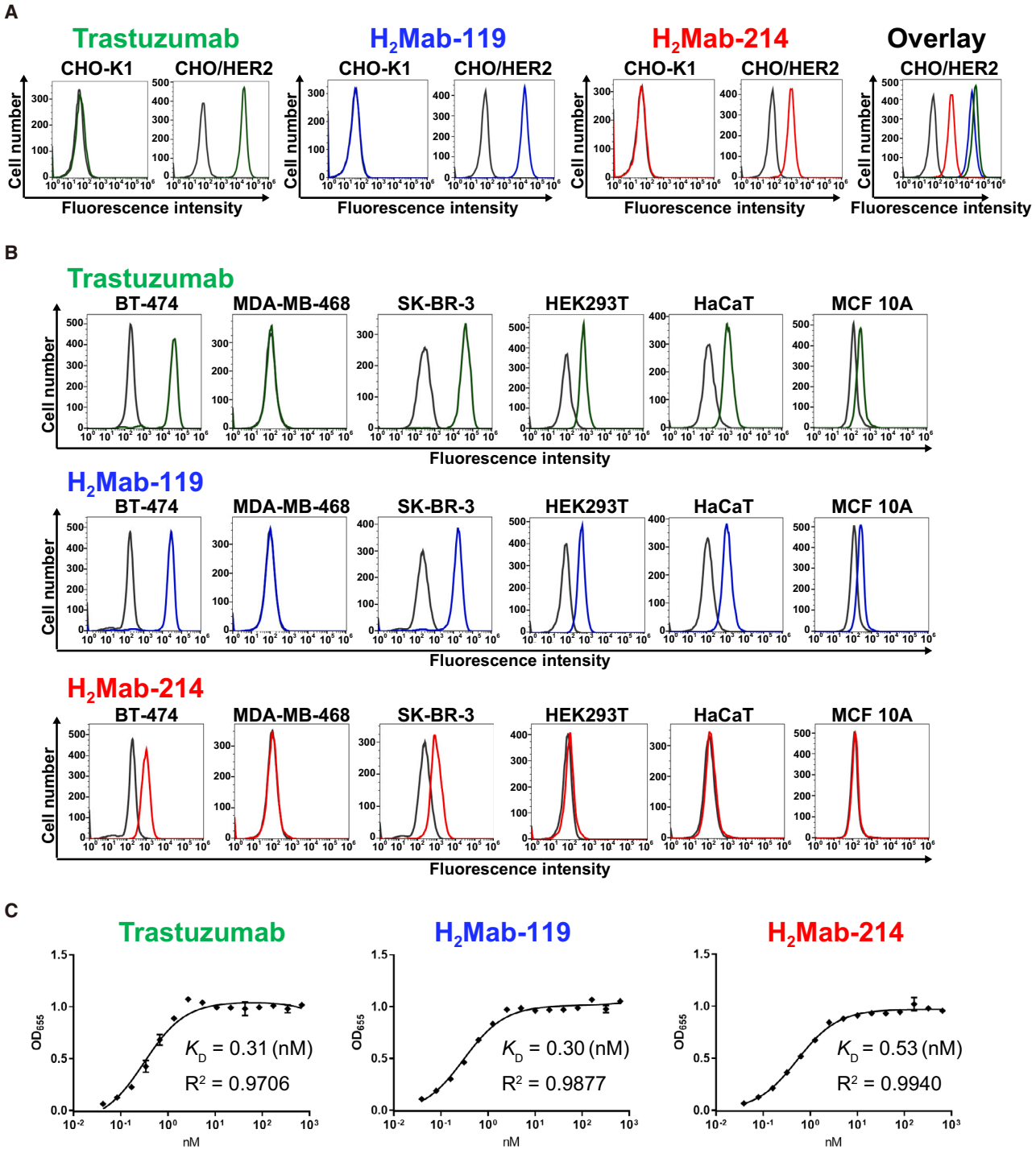

Figure 1. Binding analysis of anti-HER2 antibodies

(A) CHO-K1 and CHO/HER2 cells were treated with 10 μg/mL of trastuzumab, H_2Mab-119, and H_2Mab-214 or buffer control, and analyzed in flow cytometry.

(B) BT-474, MDA-MB-468, SK-BR-3, HEK293T, HaCaT, and MCF 10A cells were treated with 10 μg/mL of trastuzumab, H_2Mab-119, H_2Mab-214 or buffer control and analyzed in flow cytometry. The black line represents the negative control (blocking buffer).

(C) ELISA-based affinity measurement. The binding affinity of trastuzumab, H_2Mab-119, and H_2Mab-214 for HER2ec was measured by ELISA. Serially diluted antibody solutions (0.003–50 μg/mL) of each antibody were incubated with wells coated with the HER2ec, followed by incubation with peroxidase-conjugated anti-human or anti-mouse antibodies. The optical densities were measured at 655 nm and plotted. K_D values were calculated by fitting the binding isotherms using the built-in one-site binding models in GraphPad PRISM 6. Data are from a single experiment performed in duplicate (mean ± SEM).

Please cite this article in press as: Arimori et al., Locally misfolded HER2 expressed on cancer cells is a promising target for development of cancer-specific antibodies, Structure (2024), https://doi.org/10.1016/j.str.2024.02.007

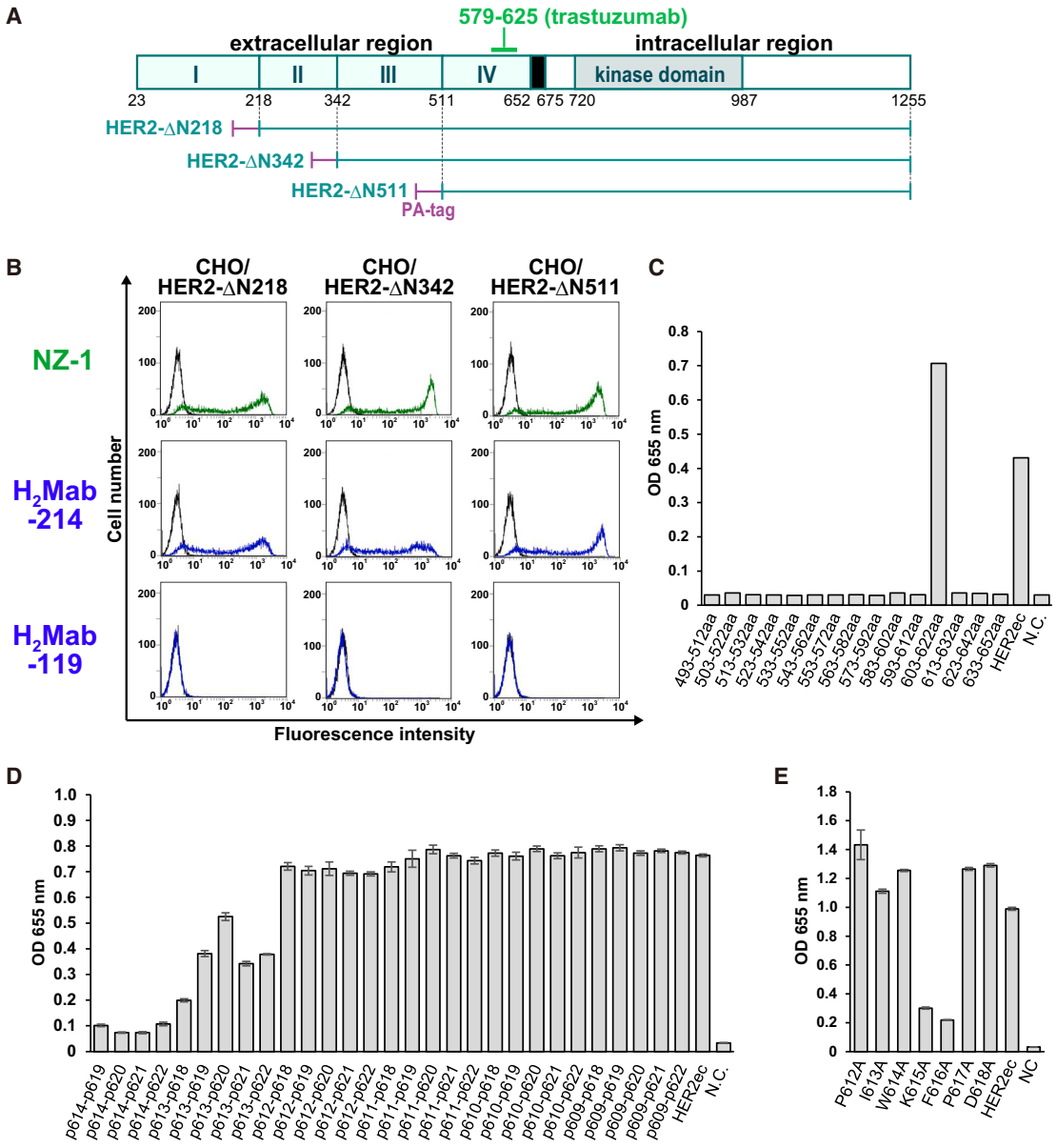

Figure 2. Epitope mapping of H_2Mab-214

(A) Domain organization of HER2 and design of a series of N-terminal domain deletion mutants used for the flow cytometry analysis.

(B) Binding of H_2Mab-214 and H_2Mab-119 to the deletion mutants of HER2 transiently expressed on CHO-K1 cells. CHO-K1 cells expressing each mutant were treated with NZ-1, H_2Mab-214, H_2Mab-119, or buffer control (black line), stained with Alexa Fluor 488-conjugated secondary antibodies, and analyzed in flow cytometry.

(C–E) Evaluation of reactivity of H_2Mab-214 toward various HER2-derived synthetic peptides by ELISA. 10 μg/mL of H_2Mab-214 was incubated with wells coated with the synthetic peptides, followed by incubation with peroxidase-conjugated anti-mouse antibodies. The optical density was measured at 655 nm. Data are from one experiment (C) or from one triplicate experiment ((D) and (E); mean ± SEM). N.C., negative control.

Epitope mapping of H_2Mab-214

Puzzled by the apparent cancer cell specificity of H_2Mab-214 in its HER2 recognition, we next explored its binding epitope. To this end, we generated a series of N-terminal deletion mutants of HER2 by successively removing domain I (ΔN218), domain II (ΔN342), and domain III (ΔN511) (Figure 2A). The comparable expression levels of these mutants on CHO-K1 cells were confirmed by the staining with NZ-1 antibody against the 16-residue PA tag attached to the N-terminus of the truncation mutants. H_2Mab-214 exhibited full reactivity toward all mutants (Figure 2B), indicating that its epitope lies exclusively within the domain IV. In contrast, the reactivity of H_2Mab-119 was completely lost upon the deletion of the domain I alone, suggesting the critical involvement of domain I in its HER2 recognition. To narrow down further the location of H_2Mab-214 epitope, we synthesized overlapping 20-mer peptides covering the domain

Please cite this article in press as: Arimori et al., Locally misfolded HER2 expressed on cancer cells is a promising target for development of cancer-specific antibodies, Structure (2024), https://doi.org/10.1016/j.str.2024.02.007

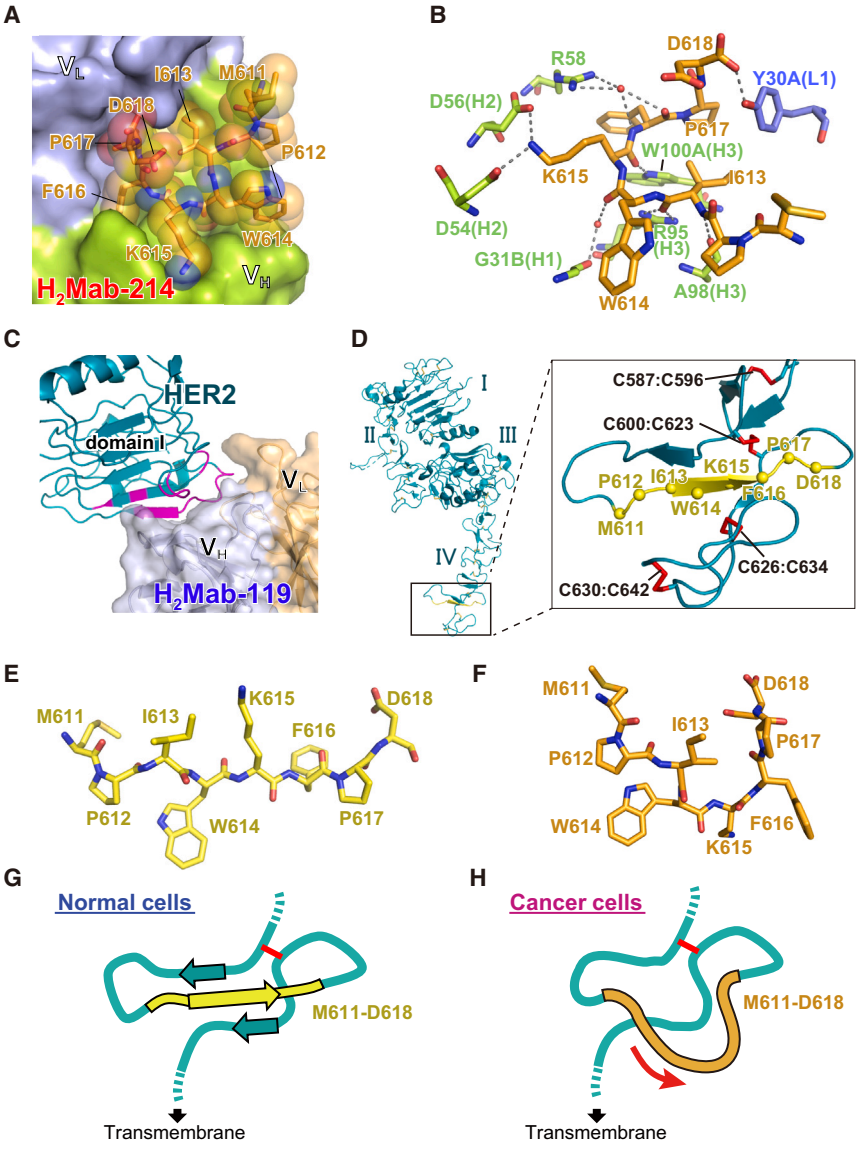

Figure 3. Structural analysis of H_2Mab-214

(A) Close-up view of the antigen binding site in the crystal structure of H_2Mab-214 complexed with the epitope peptide. H_2Mab-214 is shown as a surface model, and the epitope peptide is shown as a stick model with a transparent sphere model.

(B) Hydrogen bonding interactions observed between H_2Mab-214 and the epitope peptide. Hydrogen bonds are denoted by dashed lines. Water molecules are shown as sphere models.

(C) Crystal structure of H_2Mab-119 complexed with the HER2 domain I fragment. The domain I is shown as a cyan cartoon model, and the H_2Mab-119 is shown as a cartoon model with a transparent surface model. HER2 residues in contact with the H_2Mab-119 (within 4 Å) are indicated in magenta.

(D) Overall structure of the HER2 ectodomain (PDB ID: 3n85). Met611-Asp618 region is colored in yellow. An expanded view of the region indicated by the black box is shown on the right. The Cα atoms of the residues 611–618 are shown as spheres, and disulfide bonds are shown as red stick models.

(E–H) Structural comparison of the Met611-Asp618 region in the HER2 ectodomain ((E); crystal structure and (G); schematic diagram) and the peptide bound to H_2Mab-214 ((F); crystal structure and (H); schematic diagram). See also Figure S2.

IV and tested their reactivity by ELISA. As shown in Figure 2C, H_2Mab-214 showed strong reactivity with the peptide corresponding to residues 603–622. Subsequent analysis using the second set of shorter peptides derived from this region revealed that the linear segment Pro612-Asp618 of HER2 confers the minimally required binding epitope for H_2Mab-214 (Figure 2D). Finally, binding toward alanine-substituted HER2 peptides were evaluated to see the contribution of individual amino acid. H_2Mab-214 showed significantly reduced reactivity toward K615A and F616A peptides, indicating that Lys615 and Phe616 have major contribution to the recognition by H_2Mab-214 (Figure 2E).

Crystallographic analysis of H_2Mab-214 in complex with the epitope peptide

The epitope mapping of H_2Mab-214 revealed that it recognized linear 7-residue peptide $_{612}$-PIWKFPD-$_{618}$. This segment and the regions surrounding it are present in all major variants of HER2, and they do not contain sequence motifs suspected to undergo chemical modifications including glycosylation, phosphorylation, and deamidation (Figure S1A). Also, this segment is partially overlapped with the binding footprint of pan-HER2 reactive trastuzumab (residues 579–625) (Figure S1).[9] Therefore, it is difficult to explain the cancer specificity of H_2Mab-214 simply by cancer-specific chemical alterations or large domain-wise conformational change to expose its epitope. To understand how H_2Mab-214 distinguishes HER2 expressed on cancer cells from that on normal cells, we performed a crystallographic analysis of H_2Mab-214 in complex with its epitope peptide. To this end, antigen-binding domain of H_2Mab-214 was expressed as a small and hyper-crystallizable antibody fragment, Fv-clasp.[42] H_2Mab-214 Fv-clasp was crystallized in the presence of the excess amount of HER2 (611–618) peptide, and the complex structure was solved at 1.75 Å resolution (Table S1; Figure S2A). In the crystal structure, the Fv region has a lower average B-factor than the SARAH domain (average B-factors for the Fv and SARAH domains are 47.2 and 69.6, respectively), and a clear electron density was observed throughout. At the antigen binding site, a clear electron density corresponding to the epitope peptide was also observed, allowing us to build reliable models for all eight residues of the peptide (Figure S2B). The bound peptide is in a compact U-shaped conformation (Figure 3A), but unlike the typical turn conformation found in protein loops, it is not maintained via intramolecular main chain hydrogen bonds. Rather, the conformation is stabilized by intermolecular

Please cite this article in press as: Arimori et al., Locally misfolded HER2 expressed on cancer cells is a promising target for development of cancer-specific antibodies, Structure (2024), https://doi.org/10.1016/j.str.2024.02.007

Table 1. The main chain dihedral angles

residue	Phi/Psi angles (°) in the HER2 ectodomain structures (PDB: 3n85)	(PDB: 6j71)	Phi/Psi angles (°) in the H_2Mab-214 Fv-clasp/epitope peptide complex
Pro612	−60.9/143.0	−86.6/138.7	−62.7/149.5
Ile613	−104.1/113.8	−91.2/117.5	−106.6/102.1
Trp614	−107.3/128.4	−114.7/112.1	−76.7/-38.3
Lys615	−138.3/166.5	−133.8/170.7	−109.5/-112.4
Phe616	−141.6/152.4	−147.6/157.1	−110.6/161.9
Pro617	−78.1/160.6	−66.4/159.1	−53.0/125.4

hydrogen bonding interactions formed between the residues from the peptide and Gly31B (CDR-H1), Arg58, Arg95 (CDR-H3), Ala98 (CDR-H3), and Trp100A (CDR-H3) of H_2Mab-214 (Figure 3B). In addition, numerous inter- and intramolecular van der Waals contacts formed throughout the peptide reinforce highly complementary recognition interface that warrant high affinity for such a short stretch of amino acids (Figure 3A). Among the peptide residues, Lys615 and Phe616 appear to form particularly important interactions: the side chain of Lys615 forms salt bridges with two aspartic acid residues (Asp54 and Asp56) in CDR-H2 (Figure 3B), while the side chain of Phe616 is inserted into a deep pocket at the center of the antigen binding site and in contact with the surrounding residues (Figure 3A). These observations are in good agreement with the results of the alanine scanning (Figure 2E).

We also conducted a crystallographic analysis for the pan-HER2 antibody H_2Mab-119. As H_2Mab-119 was found to retain high binding affinity for the HER2 domain I fragment (Figure S2C), the H_2Mab-119 Fab was co-crystallized with the domain I fragment. In the complex structure solved at 1.69 Å resolution, H_2Mab-119 is in contact with two β-strands and multiple loops of the domain I, indicating that H_2Mab-119 recognizes three-dimensional (i.e., non-linear) epitope, which is in contrast to H_2Mab-214 (Figures 3C and S2D).

Structural comparison of the epitope peptide bound to H_2Mab-214 and the corresponding region in published HER2 structures

HER2 domain IV has a stalk-like structure consisting of multiple short β-sheets stabilized by ten disulfide bonds, and the H_2Mab-214 epitope sequence (Pro612 to Asp618) is located near its C-terminus (Figure 3D). So far, ten HER2 ectodomain structures containing atomic models of the epitope region have been reported (i.e., PDB IDs: 1n8z, 3be1, 3n85, 6bgt, 6j71, 6oge, 7mn5, 7mn6, 7mn8, and 8ffj), of which 3n85 and 6j71 are relatively well modeled with no disordered regions in the domain IV (Figure S2E). In all of these structures, the Pro612-Asp618 region assumes an extended conformation, with its central segment (Ile613 to Phe616) assuming a β-strand sandwiched by two strands to form a β-sheet (Figure 3D, inset), although the loop regions preceding or following it (dashed ellipses in the inset in Figure S2E) have structural diversity, some are unmodeled. This "canonical" conformation of the 612–618 segment (Figure 3E) is drastically different from the U-shaped conformation seen in the same peptide bound to H_2Mab-214 (Figure 3F). Analysis of the residue-wise main chain dihedral angles for the H_2Mab-214-captured peptide revealed large divergence from the values obtained for the published ectodomain structures, especially at Trp614, Lys615, and Phe616 (Table 1). Such fundamental difference in the conformation tells us that the 612–618 segment needs to be dislodged or "pulled-out" from the β-sheet to be recognized by H_2Mab-214, suggesting that the HER2 molecules reactive with H_2Mab-214 must undergo local unfolding near its epitope region (Figures 3G and 3H).

Effect of forced unfolding of HER2 by DTT treatment on the reactivity of anti-HER2 mAbs

Structural studies suggested that H_2Mab-214 preferentially recognizes HER2 domain IV when it is structurally compromised. However, because our crystal structure is not in complex with the HER2 ectodomain, but with the epitope peptide, we do not know whether H_2Mab-214 indeed recognizes misfolded HER2 on the cell surface. Therefore, to validate this hypothesis, we sought to artificially disrupt the tertiary structure of HER2 on normal cells and investigated antibody bindings to these cells. HER2 has many disulfide bonds in its extracellular region contributing to the overall structural stabilization at varying degree. To break the disulfide bonds of HER2 present on HEK293T cells, cells were cultured in the media containing 1 mM DTT for 1, 5, and 24 h, and reactivities of the antibody were investigated by flow cytometry (Figure 4A).[43] Remarkably, binding of H_2Mab-214 was increased more than 2-fold after the 1-h treatment with DTT, indicating that the number of epitope-bearing species increased due to the partial reduction of disulfide bonds. Furthermore, this increase was transient because the binding became less pronounced after 5 h and returned to the basal level (without DTT treatment) after 24 h. In sharp contrast, H_2Mab-119 exhibited completely opposite behavior to the DTT-treatment; the binding was reduced by >95% after 1-h DTT treatment, followed by the gradual recovery over time, returning to the basal level after 24 h (Figure 4B). These observations are consistent with the idea that brief incubation with DTT induces partial disruption of the tertiary structure of HER2, which is favored by H_2Mab-214 but disfavored by H_2Mab-119, and that the normal structure is restored as the effective concentration of DTT goes down by oxidation during the cell culture at 37°C.

To generalize the aforementioned notion, reactivities of four regular anti-HER2 mAbs, H_2Mab-19 (mouse IgG_{2b}, kappa, epitope: domain III),[44] H_2Mab-181 (mouse IgG_1, kappa, epitope: domain III),[45] H_2Mab-41 (mouse IgG_{2b}, kappa, epitope: domain IV),[46] and trastuzumab (humanized IgG_1, kappa, epitope: domain IV), with HEK293T cells were investigated 1 and 24 h after the addition of 1 mM DTT. As in the case of H_2Mab-119, all antibodies showed a markedly reduced reactivity with the cells at 1 h, and that was nearly recovered at 24 h (Figure S3). The decreased binding of non-cancer-specific mAbs with epitopes in different domains upon addition of DTT suggests that structural disruption occurred throughout the HER2 molecule. These results again highlight the unique character of H_2Mab-214 in that it recognizes structurally disrupted HER2.

If the reactivity of H_2Mab-214 is governed by the partially unfolded nature of HER2 molecules on cell surface, the DTT-induced binding upregulation should be seen in any cell types. In fact, DTT treatment of normal mammary gland epithelial cell line MCF 10A resulted in small but statistically significant ($p < 0.05$) increase in the reactivity of H_2Mab-214 (Figure 4C).

Please cite this article in press as: Arimori et al., Locally misfolded HER2 expressed on cancer cells is a promising target for development of cancer-specific antibodies, Structure (2024), https://doi.org/10.1016/j.str.2024.02.007

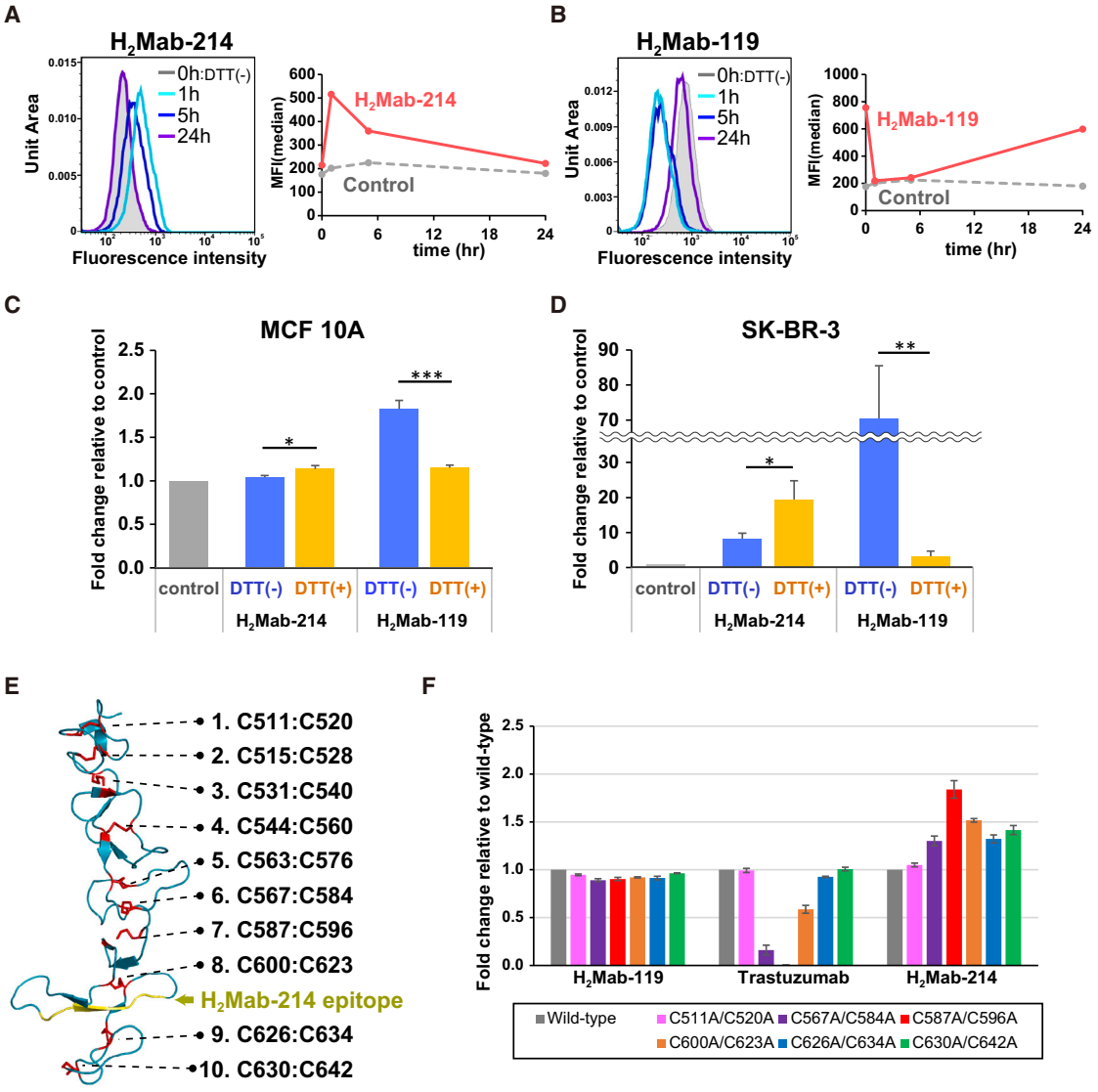

Figure 4. Analysis of antibody binding upon disulfide bond breakage in HER2

(A and B) Flow cytometry analysis of DTT-treated HEK293T cells. HEK293T cells were pre-treated with 1 mM DTT for 1, 5, or 24 h and then stained with H_2Mab-214 (A), H_2Mab-119 (B), or buffer control, followed by flow cytometry analysis. Line graphs of the median florescence intensity (MFI) values are provided on the right side of the histograms.

(C and D) Effect of DTT treatment of MCF 10A (C) and SK-BR-3 (D) cells on antibody binding. MCF 10A and SK-BR-3 cells were either untreated or pre-treated with 1 mM DTT for 1 h and then stained with H_2Mab-214, H_2Mab-119, or buffer control, followed by flow cytometry analysis. Results are reported as fold change in MFI compared with the buffer control. Data are mean +SEM of four independent experiments. p values were calculated using unpaired one-tailed t test. *$p < 0.05$, **$p < 0.01$. ***$p < 0.001$.

(E) HER2 domain IV structure extracted from 3n85. The disulfide bonds are indicated by red sticks.

(F) Binding of antibodies to the disulfide bond removal HER2 mutants. CHO-K1 cells transiently expressing each mutant were stained with H_2Mab-119, trastuzumab, or H_2Mab-214 and analyzed in flow cytometry. Relative impact of each mutation on binding is expressed as the fold change in the % positive cells from the wild-type after normalizing the expression level of each mutant using the NZ-1-stained cells. Signals from cells transfected with empty vectors were used to define antibody-bound cell populations (regions including <1% of cells transfected with empty vectors were used for the calculation of % positive cells). Data are mean ± SEM of three independent experiments. See also Figure S3.

Furthermore, the same treatment also upregulated H_2Mab-214 reactivity toward SK-BR-3 cells which were already positive for H_2Mab-214 binding before the DTT treatment (Figure 4D), indicating that there is a pool of H_2Mab-214-negative HER2 molecules expressed on breast cancer cells which can be converted to H_2Mab-214-positive ones upon DTT treatment.

Effects of targeted disruption of domain IV disulfide bond on the epitope exposure

Although the DTT treatment facilitated the conversion of HER2 domain IV to the alternative conformation reactive with H_2Mab-214, it severely reduced the binding of all other mAbs, indicating that the DTT-treated HER2 has globally disturbed structure that

Please cite this article in press as: Arimori et al., Locally misfolded HER2 expressed on cancer cells is a promising target for development of cancer-specific antibodies, Structure (2024), https://doi.org/10.1016/j.str.2024.02.007

does not accurately capture the character of H_2Mab-214-reactive species on cancer cells. Considering the fact that most anti-HER2 mAbs do not show cell-type specificity like H_2Mab-214, cancer-specific HER2 structural alteration may be restricted to domain IV, particularly the region encompassing residues 612–618. We therefore set out to investigate whether targeted local disruption of this region via removing individual disulfide linkage can mimic cancer-specific presentation of the H_2Mab-214 epitope. As the H_2Mab-214 epitope is located between the 8th and 9th disulfide bonds in the domain IV (Figure 4E), we chose to remove the 6th to 10th disulfide bonds (C567:C584, C587:C596, C600:C623, C626:C634, and C630:C642), which are relatively close to the epitope. As a control, the first disulfide bond (C511:C520) which is ~55 Å away from the epitope was also removed. To remove individual disulfide bond, the pairing cysteine residues were simultaneously replaced with alanine in the context of full-length HER2. Upon the transient expression in CHO-K1 cells, their reactivities against the anti-HER2 antibodies were evaluated by flow cytometry.

As expected, H_2Mab-119 reacted with all mutants at levels nearly equivalent to the wild-type, confirming the structural integrity at the domain I in these domain IV-mutants. Trastuzumab showed greatly reduced reactivity with the C567A/C584A and C587A/C596A mutants and moderately reduced reactivity with the C600A/C623A mutant, but binding to other mutants remained intact (Figure 4F). The epitope for trastuzumab is composed of three loops, Pro579-Gln583 (loop 1), Asp592-Phe595 (loop 2), and Lys615-Pro625 (loop 3) (Figure S1B). Structurally, the C567:C584 and C587:C596 disulfide bonds are located behind the loop 1 and 2, respectively, and appear to support the conformation of these loops, and the C600:C623 is located in a linker connecting the loop 2 and 3. Thus, the reduced binding of trastuzumab in their removal correlates well with the structural observations. When the same set of HER2 mutants were evaluated for the binding by H_2Mab-214, however, they showed increased binding at varying degrees (from 30 to 90%), except for the pair located away from the epitope (i.e., C511:C520) (Figure 4F). This result indicates that the exposure of H_2Mab-214 epitope does not require global misfolding of HER2 but can be facilitated by any local destabilization of the structure near the Pro612-Asp618 segment, which serves as a "weak ankle" of HER2 that readily changes its conformation into an alternative one. In the mutant lacking the C630:C642, where structurally the impact of the mutation appears to be small, the relatively high binding of H_2Mab-214 can be attributed not only to the disruption of the epitope conformation but also to the elongation of the conformation at the mutated site. Since the mutated site is in proximity to the membrane, this elongation might enlarge the space between the cell surface and the epitope, potentially increasing the antibody accessibility.

ADCC and CDC by H_2Mab-214-mG_{2a}-f against BT-474 and MDA-MB-468 cells

The high selectivity of H_2Mab-214 for cancer cells could be a major advantage in its pharmaceutical application. Therefore, we evaluated the potential application of H_2Mab-214 in cancer therapy. Since H_2Mab-214 is a mouse mAb (mouse IgG_1, kappa), we chose H_2Mab-119, a representative pan-HER2 mouse mAb (mouse IgG_1, kappa), as a control. Murine IgG_1 subclass antibodies have reduced binding to FcγR receptors and are closer to human IgG_4-based therapeutics, while murine IgG_{2a} are effector competent and closer to human IgG_1 antibodies.[17] Furthermore, a core fucose deficiency on the Fc *N*-glycan has been shown to enhance the Fc binding to the FcγRIIIa on the effector cells and the ADCC activity.[47] Therefore, we produced class-switched (from IgG_1 to IgG_{2a}) and defucosylated mAbs to evaluate the antitumor activity of H_2Mab-214 and H_2Mab-119. The class-switched and defucosylated mAbs (H_2Mab-214-mG_{2a}-f and H_2Mab-119-mG_{2a}-f) were produced by combining their V_H with C_H of mouse IgG_{2a} (Figure S4A). We confirmed that H_2Mab-214-mG_{2a}-f and H_2Mab-119-mG_{2a}-f recognized BT-474, but not MDA-MB-468 cells (Figure S4B). As a defucosylated control mouse IgG_{2a} mAb, we used 281-mG_{2a}-f (anti-hamster podoplanin [PDPN] mAb), which never recognized BT-474 nor MDA-MB-468 cells (Figure S4B).

We first investigated whether H_2Mab-214-mG_{2a}-f and H_2Mab-119-mG_{2a}-f could exert ADCC against BT-474 cells. Target cells (BT-474 and MDA-MB-468) were labeled with 10 μg/mL calcein AM. ADCC were determined by the calcein release into the medium after co-culture with mAbs and effector splenocytes from BALB/c nude mice. As shown in Figure 5A, H_2Mab-214-mG_{2a}-f showed ADCC activity (48.0% cytotoxicity) against BT-474 cells more potently than did the control mouse IgG_{2a} (4.4% cytotoxicity; $p < 0.01$) and 281-mG_{2a}-f (4.8% cytotoxicity; $p < 0.01$), and the activity was comparable to that induced by H_2Mab-119-mG_{2a}-f (43.6% cytotoxicity). We also investigated complement-dependent cytotoxicity (CDC) activities[48,49] of H_2Mab-214-mG_{2a}-f and H_2Mab-119-mG_{2a}-f against BT-474 cells. As shown in Figure 5B, both antibodies exhibited similar levels of CDC in BT-474 cells (H_2Mab-214-mG_{2a}-f: 76.5% cytotoxicity, H_2Mab-119-mG_{2a}-f: 72.1% cytotoxicity), which were significantly higher than that induced by control mouse IgG_{2a} (9.5% cytotoxicity; $p < 0.01$) and 281-mG_{2a}-f (17.3% cytotoxicity; $p < 0.01$). There were no differences between H_2Mab-119-mG_{2a}-f or H_2Mab-214-mG_{2a}-f and control mouse IgG_{2a} or 281-mG_{2a}-f in ADCC (Figure 5C) and CDC (Figure 5D) against MDA-MB-468 cells. These results demonstrated that H_2Mab-214-mG_{2a}-f exhibited ADCC and CDC comparable to H_2Mab-119-mG_{2a}-f against HER2-positive BT-474 cells, despite its reduced reactivity in flow cytometry (Figure 1).

Antitumor effects of H_2Mab-214-mG_{2a}-f in BT-474 xenografts

We next investigated antitumor effects of the antibodies in BT-474 xenograft mouse models. H_2Mab-119-mG_{2a}-f, H_2Mab-214-mG_{2a}-f, control normal mouse IgG, or 281-mG_{2a}-f were injected intraperitoneally on days 7, 14, and 19, after the inoculation of BT-474. The tumor volume was measured on days 7, 12, 14, 19, 22, and 26 after the inoculation. Administration of H_2Mab-119-mG_{2a}-f and H_2Mab-214-mG_{2a}-f significantly reduced tumor volume compared to that of control normal mouse IgG in the BT-474 xenograft models after days 14 and 19, respectively (Figures 6A and S5). The reduction in tumor volume on day 26 in mice treated with H_2Mab-119-mG_{2a}-f and H_2Mab-214-mG_{2a}-f was 41% and 35%, respectively, compared to mice treated with the control normal mouse IgG. In addition, as shown in Figure 6B, tumors from the H_2Mab-119-mG_{2a}-f and H_2Mab-214-mG_{2a}-f-treated mice weighed significantly

Please cite this article in press as: Arimori et al., Locally misfolded HER2 expressed on cancer cells is a promising target for development of cancer-specific antibodies, Structure (2024), https://doi.org/10.1016/j.str.2024.02.007

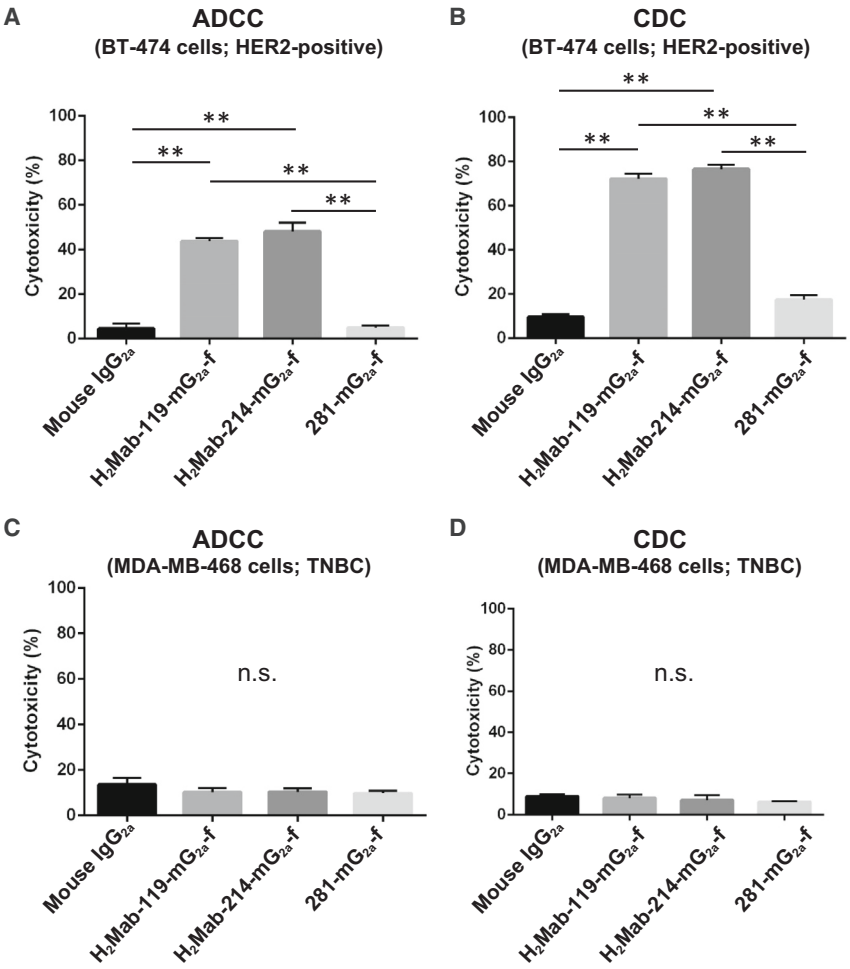

Figure 5. H_2Mab-119-mG_{2a}-f- and H_2Mab-214-mG_{2a}-f-mediated ADCC and CDC against BT-474 (HER2-positive) and MDA-MB-468 (TNBC) cells

Target cells (BT-474 and MDA-MB-468) were labeled with 10 μg/mL calcein AM. ADCC and CDC were determined by the calcein release into the medium.

(A and C) ADCC induced by H_2Mab-119-mG_{2a}-f, H_2Mab-214-mG_{2a}-f, control mouse IgG_{2a} or 281-mG_{2a}-f with effector splenocytes against BT-474 (A) and MDA-MB-468 (C) cells.

(B and D) CDC induced by H_2Mab-119-mG_{2a}-f, H_2Mab-214-mG_{2a}-f, control mouse IgG_{2a} or 281-mG_{2a}-f with complements against BT-474 (B) and MDA-MB-468 (D) cells. Values are shown as mean ± SEM. Asterisks indicate statistical significance (**$p < 0.01$; Welch's t test). ADCC, antibody-dependent cellular cytotoxicity; CDC, complement-dependent cytotoxicity.

less than those from control normal mouse IgG-treated mice (60% reduction; $p < 0.01$ and 72% reduction, respectively; $p < 0.01$). The reduction in tumor volume and weight in H_2Mab-119-mG_{2a}-f- and H_2Mab-214-mG_{2a}-f-treated mice was also significant compared to 281-mG2a-f-treated mice (Figures 6A and 6B). As a control experiment, the antitumor effects were also investigated in the MDA-MB-468 xenograft models. As a result, no difference was observed between H_2Mab-119-mG_{2a}-f or H_2Mab-214-mG_{2a}-f and control normal mouse IgG or 281-mG_{2a}-f in both tumor volume (Figure S6A) and weight (Figure S6B), confirming that the antitumor effects observed in the BT-474 xenograft models were HER2-dependent.

Tumors that were resected from mice on day 26 are demonstrated in Figures 6C and S6C. The body weight loss was not observed in both H_2Mab-119-mG_{2a}-f and H_2Mab-214-mG_{2a}-f treated mice (Figures 6D and S6D). The mice on day 26 about BT-474 xenograft and MDA-MB-468 xenograft were demonstrated in Figures S6E and S6F, respectively.

DISCUSSION

Trastuzumab is a pioneer in molecular targeted therapy and has been the most effective treatment for HER2-positive breast cancer for more than 20 years since its FDA approval in 1998.[25] The success of trastuzumab has demonstrated the utility of antibody drugs in cancer therapy, and mAbs have become one of the leading modalities in this field. As of 2018 (i.e., before COVID-19), half of the top 10 best-selling antibody drugs were reported to be against cancer.[50] More recently, attention has focused on the development of more innovative mAb-based therapeutic strategies, such as antibody-drug conjugates (ADCs), chimeric antigen receptor (CAR)-T cell therapy, and bispecific antibodies. For HER2-positive metastatic breast cancer, the ADCs, trastuzumab emtansine and trastuzumab deruxtecan, have already been developed. With the trend shifting toward such therapies with high cell-killing activity, antibodies with high specificity for cancer cells are becoming increasingly important. In the development of therapeutic antibodies against cancers, efforts are being made to identify unique characteristics of cancer cells. A major strategy is to identify molecules that are highly expressed on the surface of certain types of cancer cells and have a high cancer cell/normal cell ratio as HER2. However, many of the molecules that are abnormally expressed on cancer cells have already been identified by extensive transcriptome and proteome analyses, making exploration for new cancer antigens very challenging. In addition, in this strategy, the target molecules are common autoantigens that are also expressed on normal cells, raising concerns about adverse effects caused by antibody drugs.

In this study, we succeeded in developing the cancer-specific mAb targeting HER2. In the cell lines examined here, the reactivity of H_2Mab-214 against cancer cells was clearly observed, whereas that against normal cells was not detectable even by flow cytometry, a highly sensitive detection system (Figure 1). Since we evaluated only a limited number of cell types, further investigation is needed to determine whether H_2Mab-214 exhibits selectivity against various types of HER2-positive cancer cells. Our structural and cell-based binding analyses strongly suggested that the

Please cite this article in press as: Arimori et al., Locally misfolded HER2 expressed on cancer cells is a promising target for development of cancer-specific antibodies, Structure (2024), https://doi.org/10.1016/j.str.2024.02.007

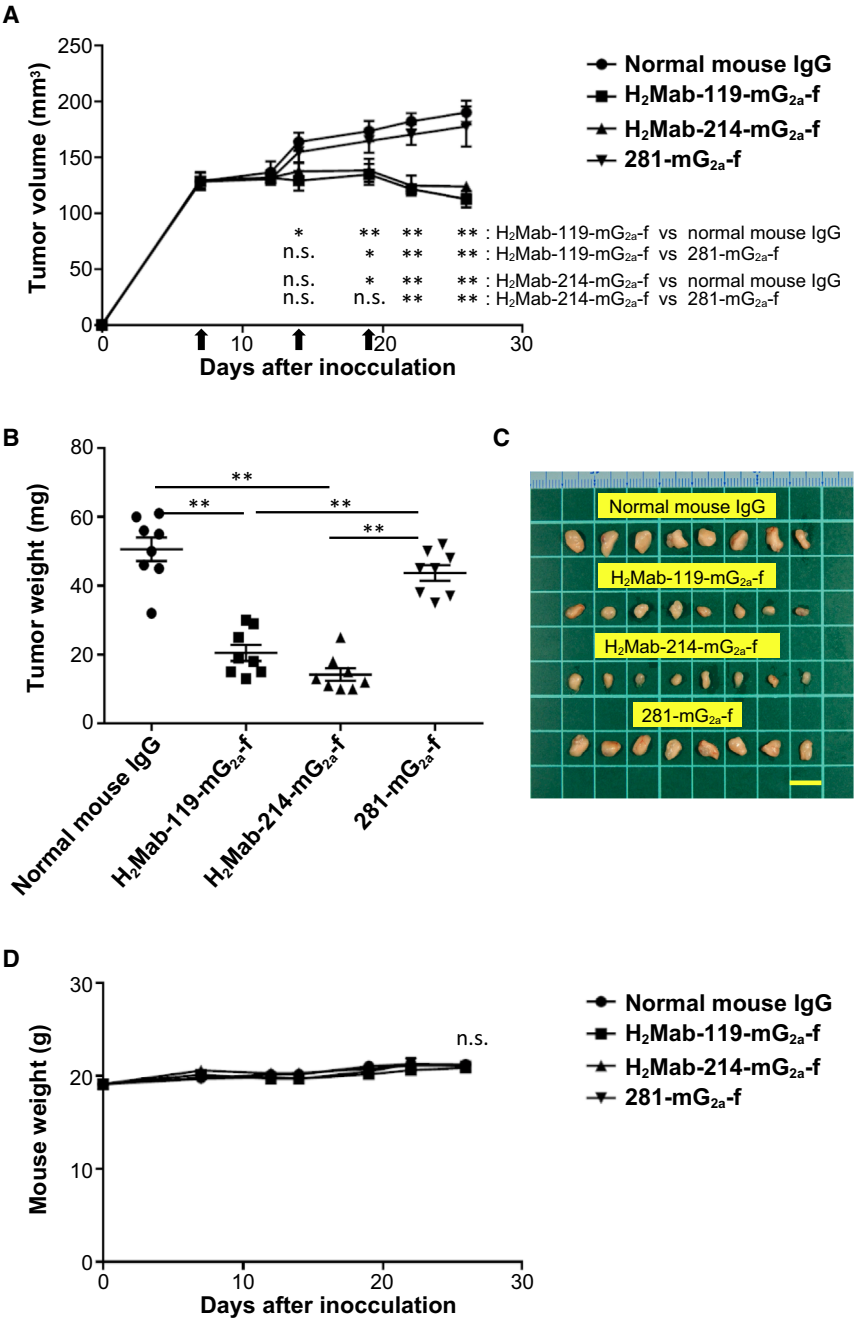

Figure 6. Antitumor activity of H_2Mab-119-mG_{2a}-f and H_2Mab-214-mG_{2a}-f against BT-474 xenograft

(A) BT-474 cells (5 × 10^6 cells) were subcutaneously injected into BALB/c nude mice. On day 7 (arrow), H_2Mab-119-mG_{2a}-f (n = 8), H_2Mab-214-mG_{2a}-f (n = 8), control normal mouse IgG (n = 8), or 281-mG_{2a}-f (n = 8) were injected intraperitoneally into mice (5 mg/kg). Additional antibodies were injected on days 14 and 19 (arrows). The tumor volume was measured on days 7, 12, 14, 19, 22, and 26 after the inoculation of BT-474. Values are presented as the mean ± SEM. *p < 0.05, **p < 0.01 (ANOVA and Tukey's multiple comparisons test).

(B) Tumor weight (day 26) was measured from excised BT-474 xenograft tumors. Values are presented as the mean ± SEM. **p < 0.01 (Welch's t test).

(C) Appearance of BT-474 xenograft tumors from the H_2Mab-119-mG_{2a}-f, H_2Mab-214-mG_{2a}-f, control normal mouse IgG and 281-mG_{2a}-f-treated mice on day 26 (scale bar, 1 cm).

(D) Mice weight in H_2Mab-119-mG_{2a}-f, H_2Mab-214-mG_{2a}-f, control normal mouse IgG and 281-mG_{2a}-f-treated groups. n.s., not significant. See also Figures S5 and S6.

preferential binding of H_2Mab-214 to cancer cells is due to the recognition of a structural feature that only HER2 on cancer cells has, namely the misfolded region. Previously, cancer-specific antibodies that appear to recognize structural features of target molecules, anti-EGFR antibody mAb806 and anti-α4β7 integrin antibody MMG49, have been reported.[51,52] Their cancer specificity is, however, thought to be linked to the global conformation of their target molecules rather than to local structural features. More specifically, their epitopes are expected to be hidden on normal cells but exposed on cancer cells for some reason. For mAb806, it has also been demonstrated by crystallographic analysis that the antigen peptide bound to the antibody has almost the same conformation as the corresponding region in the EGFR.[53] By contrast, H_2Mab-214 is a new type of cancer-specific mAb that directly recognizes the unique structural feature of the target. In the current crystal structure, the epitope peptide (Met611-Asp618) assumes U-shaped conformation nestled in the binding pocket of H_2Mab-214. This is not compatible with the canonical conformation observed in native HER2 reported so far. As the segment is part of a rigid 3-strand β-sheet in the native structure, the HER2 species reactive with H_2Mab-214 must have undergone local misfolding at this region to allow the access of the antibody. Therefore, H_2Mab-214-reactive HER2 on cancer cells and H_2Mab-214-non-reactive HER2 on normal cells are chemically identical molecules having a subtle conformational difference present in a restricted region near the Pro612-Asp618 (Figures 3G and 3H). Although we cannot rule out the possibility that such misfolding transiently occurs in a minor population of HER2 molecules on normal cells, the cancer-specific misfolding of the Pro612-Asp618 segment appears to give special advantage of cancer selectivity to H_2Mab-214, particularly when combined with the high total number of the HER2 molecule on HER2-positive cancer cells.

Proteins are inherently prone to misfolding. Homeostasis of membrane and secretory proteins is normally maintained by quality control system in the endoplasmic reticulum (ER), but cancer cells are constantly exposed to a variety of stressors such as oxidative stress, hypoxia, and decreased energy supply,

which are known to promote production and accumulation of misfolded proteins in the ER (called ER stress).[54] We speculate that in such an abnormal condition of the ER in cancer cells, proteins with minor structural defects (such as a misformation of a disulfide bond that does not impair overall domain stability or function) may escape the quality control system and are transported normally, presenting a cancer-specific "mark" to the immune system. Since our study showed that the conformational integrity of HER2 at residues 612 to 618 is susceptible to the lack of surrounding disulfide bonds, the local misfolding of HER2 may have stemmed from the disregulated redox system in the ER of cancer cells. In breast cancer cells, it has been reported that the expression of protein disulfide isomerases (PDI), PDIA1, PDIA3, PDIA4, and PDIA6, is elevated, suggesting an abnormal state of the redox system in the ER.[55] Disruption of disulfide bond formation in cancer cells has also been proposed for EGFR.[53]

As far as we are aware, only H_2Mab-214 shows cancer specificity among the many anti-HER2 antibodies developed to date, including trastuzumab that recognizes a region very close to the H_2Mab-214 epitope. Therefore, the H_2Mab-214 epitope (Pro612-Asp618 region) may be very special in that it undergoes spatially confined misfolding to expose highly antigenic peptide in cancer cells. Surprisingly, when we immunized mice with a synthetic peptide containing the H_2Mab-214 epitope sequence, all mAbs obtained were found to show cancer specificity (data not shown). This suggests that prior knowledge about the misfold-dependent cancer neoantigen sequence may be leveraged to obtain useful cancer-specific mAbs. By using such strategy, it may be possible to establish H_2Mab-214-like antibodies that are more suitable for therapeutic applications, such as fully human mAbs and high-affinity mAbs. As evidenced by the performance of trastuzumab, the lower stalk region of HER2 should be a promising target in terms of the therapeutic efficacy as well. In fact, even though not all HER2 molecules on cancer cells are H_2Mab-214 reactive, H_2Mab-214 showed anti-tumor activity comparable to the pan-HER2 reactive H_2Mab-119 (Figures 4 and 6). Since this study used a human breast cancer xenograft model in nude mice which lack intact immunity, further studies using syngeneic model of HER2-expressing murine breast cancers are needed to evaluate the contribution of whole immune system.

HER2 has a long history as a successful cancer therapeutic target and has been well studied, yet its unique and cancer-specific structural defect that can be targeted by mAb had not been discovered until now. Our results indicate that some molecules that had not been considered as good cancer-specific therapeutic target due to the widespread expression in many tissues may in fact become viable drug target if they are found to undergo cancer-specific local misfolding. It is hoped that the expansion of potential targets will facilitate the development of mAb therapies for cancers for which effective treatments have not yet been found.

STAR★METHODS

Detailed methods are provided in the online version of this paper and include the following:

- KEY RESOURCES TABLE
- RESOURCE AVAILABILITY
  - Lead contact
  - Materials availability
  - Data and code availability
- EXPERIMENTAL MODEL AND STUDY PARTICIPANT DETAILS
  - Cell lines
  - Animals
- METHOD DETAILS
  - Antibodies
  - Flow cytometry
  - Enzyme-linked immunosorbent assay (ELISA)
  - ADCC
  - CDC
  - Antitumor activity of H_2Mab-119-mG2a-f and H_2Mab-214-mG_{2a}-f in xenografts of BT-474 and MDA-MB-468 cells
  - Crystallization
  - Data collection, structure determination, and refinement
- QUANTIFICATION AND STATISTICAL ANALYSIS

SUPPLEMENTAL INFORMATION

Supplemental information can be found online at https://doi.org/10.1016/j.str.2024.02.007.

ACKNOWLEDGMENTS

We would like to thank the staff of the beamline at SPring-8 for their help with X-ray data collection. This work was supported in part by JSPS KAKENHI grant numbers JP21H02416 to T.A. and JP22K07224 to Y.K. from Japan Society for the Promotion of Science, by the Research Support Project for Life Science and Drug Discovery (Basis for Supporting Innovative Drug Discovery and Life Science Research [BINDS]) from Japan Agency for Medical Research and Development (AMED) under grant numbers JP22ama121011 to J.T. and JP22ama121008 to Y.K., and also supported by AMED under grant numbers JP22am0401013 to Y.K., 23bm1123027h0001 to Y.K., and JP22ck0106730 to Y.K.

AUTHOR CONTRIBUTIONS

T.A. designed and performed experiments, analyzed the data, and wrote the manuscript. E.M., H.S., T.O., T.T., and M.K.K. performed experiments and analyzed the data. J.T. and Y.K. conceived the experimental design, analyzed the data, and wrote the manuscript. All authors contributed to the preparation of the manuscript.

DECLARATION OF INTERESTS

M.K.K. and Y.K. submitted a patent application related to this work: H_2Mab-214. Patent application number WO2022114163. (2021).

Received: August 20, 2023
Revised: January 10, 2024
Accepted: February 13, 2024
Published: March 8, 2024

REFERENCES

1. Yarden, Y., and Sliwkowski, M.X. (2001). Untangling the ErbB signalling network. Nat. Rev. Mol. Cell Biol. *2*, 127–137. https://doi.org/10.1038/35052073.
2. Cho, H.S., and Leahy, D.J. (2002). Structure of the extracellular region of HER3 reveals an interdomain tether. Science *297*, 1330–1333. https://doi.org/10.1126/science.1074611.

3. Ferguson, K.M., Berger, M.B., Mendrola, J.M., Cho, H.S., Leahy, D.J., and Lemmon, M.A. (2003). EGF activates its receptor by removing interactions that autoinhibit ectodomain dimerization. Mol. Cell *11*, 507–517. https://doi.org/10.1016/s1097-2765(03)00047-9.

4. Bouyain, S., Longo, P.A., Li, S., Ferguson, K.M., and Leahy, D.J. (2005). The extracellular region of ErbB4 adopts a tethered conformation in the absence of ligand *102*, 15024–15029. https://doi.org/10.1073/pnas.0507591102.

5. Ogiso, H., Ishitani, R., Nureki, O., Fukai, S., Yamanaka, M., Kim, J.H., Saito, K., Sakamoto, A., Inoue, M., Shirouzu, M., and Yokoyama, S. (2002). Crystal structure of the complex of human epidermal growth factor and receptor extracellular domains. Cell *110*, 775–787. https://doi.org/10.1016/s0092-8674(02)00963-7.

6. Garrett, T.P.J., McKern, N.M., Lou, M., Elleman, T.C., Adams, T.E., Lovrecz, G.O., Zhu, H.J., Walker, F., Frenkel, M.J., Hoyne, P.A., et al. (2002). Crystal structure of a truncated epidermal growth factor receptor extracellular domain bound to transforming growth factor alpha. Cell *110*, 763–773. https://doi.org/10.1016/s0092-8674(02)00940-6.

7. Liu, P., Cleveland, T.E., 4th, Bouyain, S., Byrne, P.O., Longo, P.A., and Leahy, D.J. (2012). A single ligand is sufficient to activate EGFR dimers *109*, 10861–10866. https://doi.org/10.1073/pnas.1201114109.

8. Cho, H.S., Mason, K., Ramyar, K.X., Stanley, A.M., Gabelli, S.B., Denney, D.W., Jr., and Leahy, D.J. (2003). Structure of the extracellular region of HER2 alone and in complex with the Herceptin Fab. Nature *421*, 756–760. https://doi.org/10.1038/nature01392.

9. Diwanji, D., Trenker, R., Thaker, T.M., Wang, F., Agard, D.A., Verba, K.A., and Jura, N. (2021). Structures of the HER2-HER3-NRG1beta complex reveal a dynamic dimer interface. Nature *600*, 339–343. https://doi.org/10.1038/s41586-021-04084-z.

10. Citri, A., and Yarden, Y. (2006). EGF-ERBB signalling: towards the systems level. Nat. Rev. Mol. Cell Biol. *7*, 505–516. https://doi.org/10.1038/nrm1962.

11. Rimawi, M.F., Schiff, R., and Osborne, C.K. (2015). Targeting HER2 for the treatment of breast cancer. Annu. Rev. Med. *66*, 111–128. https://doi.org/10.1146/annurev-med-042513-015127.

12. Slamon, D.J., Clark, G.M., Wong, S.G., Levin, W.J., Ullrich, A., and McGuire, W.L. (1987). Human breast cancer: correlation of relapse and survival with amplification of the HER-2/neu oncogene. Science *235*, 177–182. https://doi.org/10.1126/science.3798106.

13. Van Cutsem, E., Bang, Y.J., Feng-Yi, F., Xu, J.M., Lee, K.W., Jiao, S.C., Chong, J.L., López-Sanchez, R.I., Price, T., Gladkov, O., et al. (2015). HER2 screening data from ToGA: targeting HER2 in gastric and gastro-esophageal junction cancer. Gastric Cancer *18*, 476–484. https://doi.org/10.1007/s10120-014-0402-y.

14. Slamon, D.J., Godolphin, W., Jones, L.A., Holt, J.A., Wong, S.G., Keith, D.E., Levin, W.J., Stuart, S.G., Udove, J., Ullrich, A., et al. (1989). Studies of the HER-2/neu proto-oncogene in human breast and ovarian cancer. Science *244*, 707–712. https://doi.org/10.1126/science.2470152.

15. Schneider, P.M., Hung, M.C., Chiocca, S.M., Manning, J., Zhao, X.Y., Fang, K., and Roth, J.A. (1989). Differential expression of the c-erbB-2 gene in human small cell and non-small cell lung cancer. Cancer Res. *49*, 4968–4971.

16. Zhau, H.E., Zhang, X., von Eschenbach, A.C., Scorsone, K., Babaian, R.J., Ro, J.Y., and Hung, M.C. (1990). Amplification and expression of the c-erb B-2/neu proto-oncogene in human bladder cancer. Mol. Carcinog. *3*, 254–257. https://doi.org/10.1002/mc.2940030503.

17. Tsao, L.C., Force, J., and Hartman, Z.C. (2021). Mechanisms of Therapeutic Antitumor Monoclonal Antibodies. Cancer Res. *81*, 4641–4651. https://doi.org/10.1158/0008-5472.CAN-21-1109.

18. Essadi, I., Benbrahim, Z., Kaakoua, M., Reverdy, T., Corbaux, P., and Freyer, G. (2023). HER2-Positive Metastatic Breast Cancer: Available Treatments and Current Developments. Cancers *15*, 1738. https://doi.org/10.3390/cancers15061738.

19. Slamon, D.J., Leyland-Jones, B., Shak, S., Fuchs, H., Paton, V., Bajamonde, A., Fleming, T., Eiermann, W., Wolter, J., Pegram, M., et al. (2001). Use of chemotherapy plus a monoclonal antibody against HER2 for metastatic breast cancer that overexpresses HER2. N. Engl. J. Med. *344*, 783–792. https://doi.org/10.1056/nejm200103153441101.

20. Bang, Y.J., Van Cutsem, E., Feyereislova, A., Chung, H.C., Shen, L., Sawaki, A., Lordick, F., Ohtsu, A., Omuro, Y., Satoh, T., et al. (2010). Trastuzumab in combination with chemotherapy versus chemotherapy alone for treatment of HER2-positive advanced gastric or gastro-oesophageal junction cancer (ToGA): a phase 3, open-label, randomised controlled trial. Lancet *376*, 687–697. https://doi.org/10.1016/s0140-6736(10)61121-x.

21. Musolino, A., Gradishar, W.J., Rugo, H.S., Nordstrom, J.L., Rock, E.P., Arnaldez, F., and Pegram, M.D. (2022). Role of Fcγ receptors in HER2-targeted breast cancer therapy. J. Immunother. Cancer *10*, e003171. https://doi.org/10.1136/jitc-2021-003171.

22. Nordstrom, J.L., Gorlatov, S., Zhang, W., Yang, Y., Huang, L., Burke, S., Li, H., Ciccarone, V., Zhang, T., Stavenhagen, J., et al. (2011). Anti-tumor activity and toxicokinetics analysis of MGAH22, an anti-HER2 monoclonal antibody with enhanced Fcγ receptor binding properties. Breast Cancer Res. *13*, R123. https://doi.org/10.1186/bcr3069.

23. McAndrew, N.P. (2022). Updates on targeting human epidermal growth factor receptor 2-positive breast cancer: what's to know in 2021. Curr. Opin. Obstet. Gynecol. *34*, 41–45. https://doi.org/10.1097/gco.0000000000000762.

24. Rugo, H.S., Im, S.A., Cardoso, F., Cortés, J., Curigliano, G., Musolino, A., Pegram, M.D., Wright, G.S., Saura, C., Escrivá-de-Romaní, S., et al. (2021). Efficacy of Margetuximab vs Trastuzumab in Patients With Pretreated ERBB2-Positive Advanced Breast Cancer: A Phase 3 Randomized Clinical Trial. JAMA Oncol. *7*, 573–584. https://doi.org/10.1001/jamaoncol.2020.7932.

25. Maadi, H., Soheilifar, M.H., Choi, W.S., Moshtaghian, A., and Wang, Z. (2021). Trastuzumab Mechanism of Action; 20 Years of Research to Unravel a Dilemma. Cancers *13*, 3540. https://doi.org/10.3390/cancers13143540.

26. Gala, K., and Chandarlapaty, S. (2014). Molecular pathways: HER3 targeted therapy. Clin. Cancer Res. *20*, 1410–1416. https://doi.org/10.1158/1078-0432.CCR-13-1549.

27. Franklin, M.C., Carey, K.D., Vajdos, F.F., Leahy, D.J., de Vos, A.M., and Sliwkowski, M.X. (2004). Insights into ErbB signaling from the structure of the ErbB2-pertuzumab complex. Cancer Cell *5*, 317–328. https://doi.org/10.1016/s1535-6108(04)00083-2.

28. Badache, A., and Hynes, N.E. (2004). A new therapeutic antibody masks ErbB2 to its partners. Cancer Cell *5*, 299–301. https://doi.org/10.1016/s1535-6108(04)00088-1.

29. Swain, S.M., Baselga, J., Kim, S.B., Ro, J., Semiglazov, V., Campone, M., Ciruelos, E., Ferrero, J.M., Schneeweiss, A., Heeson, S., et al. (2015). Pertuzumab, trastuzumab, and docetaxel in HER2-positive metastatic breast cancer. N. Engl. J. Med. *372*, 724–734. https://doi.org/10.1056/NEJMoa1413513.

30. Copeland-Halperin, R.S., Liu, J.E., and Yu, A.F. (2019). Cardiotoxicity of HER2-targeted therapies. Curr. Opin. Cardiol. *34*, 451–458. https://doi.org/10.1097/hco.0000000000000637.

31. Lee, K.F., Simon, H., Chen, H., Bates, B., Hung, M.C., and Hauser, C. (1995). Requirement for neuregulin receptor erbB2 in neural and cardiac development. Nature *378*, 394–398. https://doi.org/10.1038/378394a0.

32. Crone, S.A., Zhao, Y.Y., Fan, L., Gu, Y., Minamisawa, S., Liu, Y., Peterson, K.L., Chen, J., Kahn, R., Condorelli, G., et al. (2002). ErbB2 is essential in the prevention of dilated cardiomyopathy. Nat. Med. *8*, 459–465. https://doi.org/10.1038/nm0502-459.

33. Wang, D., Eraslan, B., Wieland, T., Hallström, B., Hopf, T., Zolg, D.P., Zecha, J., Asplund, A., Li, L.H., Meng, C., et al. (2019). A deep proteome and transcriptome abundance atlas of 29 healthy human tissues. Mol. Syst. Biol. *15*, e8503. https://doi.org/10.15252/msb.20188503.

34. Kato, Y., and Kaneko, M.K. (2014). A cancer-specific monoclonal antibody recognizes the aberrantly glycosylated podoplanin. Sci. Rep. *4*, 5924. https://doi.org/10.1038/srep05924.

35. Yamada, S., Ogasawara, S., Kaneko, M.K., and Kato, Y. (2017). LpMab-23: A Cancer-Specific Monoclonal Antibody Against Human Podoplanin. Monoclon. Antibodies Immunodiagn. Immunother. *36*, 72–76. https://doi.org/10.1089/mab.2017.0001.

36. Kaneko, M.K., Ohishi, T., Kawada, M., and Kato, Y. (2020). A cancer-specific anti-podocalyxin monoclonal antibody (60-mG(2a)-f) exerts anti-tumor effects in mouse xenograft models of pancreatic carcinoma. Biochem. Biophys. Rep. *24*, 100826. https://doi.org/10.1016/j.bbrep.2020.100826.

37. Suzuki, H., Kaneko, M.K., and Kato, Y. (2022). Roles of Podoplanin in Malignant Progression of Tumor. Cells *11*. https://doi.org/10.3390/cells11030575.

38. Yamada, S., Itai, S., Nakamura, T., Chang, Y.W., Harada, H., Suzuki, H., Kaneko, M.K., and Kato, Y. (2017). Establishment of H(2)Mab-119, an Anti-Human Epidermal Growth Factor Receptor 2 Monoclonal Antibody, Against Pancreatic Cancer. Monoclon. Antibodies Immunodiagn. Immunother. *36*, 287–290. https://doi.org/10.1089/mab.2017.0050.

39. Kumar, R., Shepard, H.M., and Mendelsohn, J. (1991). Regulation of phosphorylation of the c-erbB-2/HER2 gene product by a monoclonal antibody and serum growth factor(s) in human mammary carcinoma cells. Mol. Cell Biol. *11*, 979–986. https://doi.org/10.1128/mcb.11.2.979-986.1991.

40. Roetger, A., Merschjann, A., Dittmar, T., Jackisch, C., Barnekow, A., and Brandt, B. (1998). Selection of potentially metastatic subpopulations expressing c-erbB-2 from breast cancer tissue by use of an extravasation model. Am. J. Pathol. *153*, 1797–1806. https://doi.org/10.1016/S0002-9440(10)65694-5.

41. Troise, F., Cafaro, V., Giancola, C., D'Alessio, G., and De Lorenzo, C. (2008). Differential binding of human immunoagents and Herceptin to the ErbB2 receptor. FEBS J. *275*, 4967–4979. https://doi.org/10.1111/j.1742-4658.2008.06625.x.

42. Arimori, T., Kitago, Y., Umitsu, M., Fujii, Y., Asaki, R., Tamura-Kawakami, K., and Takagi, J. (2017). Fv-clasp: An Artificially Designed Small Antibody Fragment with Improved Production Compatibility, Stability, and Crystallizability. Structure *25*, 1611–1622.e4. https://doi.org/10.1016/j.str.2017.08.011.

43. Ni, H., Li, A., Simonsen, N., and Wilkins, J.A. (1998). Integrin activation by dithiothreitol or Mn2+ induces a ligand-occupied conformation and exposure of a novel NH2-terminal regulatory site on the beta1 integrin chain. J. Biol. Chem. *273*, 7981–7987. https://doi.org/10.1074/jbc.273.14.7981.

44. Takei, J., Kaneko, M.K., Ohishi, T., Kawada, M., Harada, H., and Kato, Y. (2020). H(2)Mab-19, an anti-human epidermal growth factor receptor 2 monoclonal antibody exerts antitumor activity in mouse oral cancer xenografts. Exp. Ther. Med. *20*, 846–853. https://doi.org/10.3892/etm.2020.8765.

45. Asano, T., Takei, J., Suzuki, H., Kaneko, M.K., and Kato, Y. (2021). Epitope Mapping of an Anti-HER2 Monoclonal Antibody (H(2)Mab-181) Using Enzyme-Linked Immunosorbent Assay. Monoclon. Antibodies Immunodiagn. Immunother. *40*, 255–260. https://doi.org/10.1089/mab.2021.0029.

46. Kato, Y., Ohishi, T., Yamada, S., Itai, S., Takei, J., Sano, M., Nakamura, T., Harada, H., Kawada, M., and Kaneko, M.K. (2019). Anti-Human Epidermal Growth Factor Receptor 2 Monoclonal Antibody H(2)Mab-41 Exerts Antitumor Activity in a Mouse Xenograft Model of Colon Cancer. Monoclon. Antibodies Immunodiagn. Immunother. *38*, 157–161. https://doi.org/10.1089/mab.2019.0017.

47. Shinkawa, T., Nakamura, K., Yamane, N., Shoji-Hosaka, E., Kanda, Y., Sakurada, M., Uchida, K., Anazawa, H., Satoh, M., Yamasaki, M., et al. (2003). The absence of fucose but not the presence of galactose or bisecting N-acetylglucosamine of human IgG1 complex-type oligosaccharides shows the critical role of enhancing antibody-dependent cellular cytotoxicity. J. Biol. Chem. *278*, 3466–3473. https://doi.org/10.1074/jbc.M210665200.

48. Golay, J., and Taylor, R.P. (2020). The Role of Complement in the Mechanism of Action of Therapeutic Anti-Cancer mAbs. Antibodies *9*, 58. https://doi.org/10.3390/antib9040058.

49. Reis, E.S., Mastellos, D.C., Ricklin, D., Mantovani, A., and Lambris, J.D. (2018). Complement in cancer: untangling an intricate relationship. Nat. Rev. Immunol. *18*, 5–18. https://doi.org/10.1038/nri.2017.97.

50. Lu, R.M., Hwang, Y.C., Liu, I.J., Lee, C.C., Tsai, H.Z., Li, H.J., and Wu, H.C. (2020). Development of therapeutic antibodies for the treatment of diseases. J. Biomed. Sci. *27*, 1. https://doi.org/10.1186/s12929-019-0592-z.

51. Scott, A.M., Lee, F.T., Tebbutt, N., Herbertson, R., Gill, S.S., Liu, Z., Skrinos, E., Murone, C., Saunder, T.H., Chappell, B., et al. (2007). A phase I clinical trial with monoclonal antibody ch806 targeting transitional state and mutant epidermal growth factor receptors *104*, 4071–4076. https://doi.org/10.1073/pnas.0611693104.

52. Hosen, N., Matsunaga, Y., Hasegawa, K., Matsuno, H., Nakamura, Y., Makita, M., Watanabe, K., Yoshida, M., Satoh, K., Morimoto, S., et al. (2017). The activated conformation of integrin beta7 is a novel multiple myeloma-specific target for car T cell therapy. Nat. Med. *23*, 1436–1443. https://doi.org/10.1038/nm.4431.

53. Garrett, T.P.J., Burgess, A.W., Gan, H.K., Luwor, R.B., Cartwright, G., Walker, F., Orchard, S.G., Clayton, A.H.A., Nice, E.C., Rothacker, J., et al. (2009). Antibodies specifically targeting a locally misfolded region of tumor associated EGFR *106*, 5082–5087. https://doi.org/10.1073/pnas.0811559106.

54. Oakes, S.A. (2020). Endoplasmic Reticulum Stress Signaling in Cancer Cells. Am. J. Pathol. *190*, 934–946. https://doi.org/10.1016/j.ajpath.2020.01.010.

55. Powell, L.E., and Foster, P.A. (2021). Protein disulphide isomerase inhibition as a potential cancer therapeutic strategy. Cancer Med. *10*, 2812–2825. https://doi.org/10.1002/cam4.3836.

56. Kato, Y., Kaneko, M.K., Kuno, A., Uchiyama, N., Amano, K., Chiba, Y., Hasegawa, Y., Hirabayashi, J., Narimatsu, H., Mishima, K., and Osawa, M. (2006). Inhibition of tumor cell-induced platelet aggregation using a novel anti-podoplanin antibody reacting with its platelet-aggregation-stimulating domain. Biochem. Biophys. Res. Commun. *349*, 1301–1307. https://doi.org/10.1016/j.bbrc.2006.08.171.

57. Suzuki, H., Ohishi, T., Asano, T., Tanaka, T., Saito, M., Mizuno, T., Yoshikawa, T., Kawada, M., Kaneko, M.K., and Kato, Y. (2022). Defucosylated mouse-dog chimeric anti-HER2 monoclonal antibody exerts antitumor activities in mouse xenograft models of canine tumors. Oncol. Rep. *48*, 154. https://doi.org/10.3892/or.2022.8366.

58. Kaneko, M., Kato, Y., Horiuchi, H., and Osawa, M. (2003). Molecular characterization of a human monoclonal antibody to B antigen in ABO blood type. Immunol. Lett. *86*, 45–51. https://doi.org/10.1016/s0165-2478(02)00294-8.

59. Li, G., Suzuki, H., Ohishi, T., Asano, T., Tanaka, T., Yanaka, M., Nakamura, T., Yoshikawa, T., Kawada, M., Kaneko, M.K., and Kato, Y. (2023). Antitumor activities of a defucosylated anti-EpCAM monoclonal antibody in colorectal carcinoma xenograft models. Int. J. Mol. Med. *51*, 18. https://doi.org/10.3892/ijmm.2023.5221.

60. Kabsch, W. (2010). Acta Crystallogr. D Biol. Crystallogr. *66*, 125–132. https://doi.org/10.1107/S0907444909047337.

61. Mccoy, A.J., Grosse-Kunstleve, R.W., Adams, P.D., Winn, M.D., Storoni, L.C., and Read, R.J. (2007). Phaser crystallographic software. J. Appl. Crystallogr. *40*, 658–674. https://doi.org/10.1107/S0021889807021206.

62. Winn, M.D., Ballard, C.C., Cowtan, K.D., Dodson, E.J., Emsley, P., Evans, P.R., Keegan, R.M., Krissinel, E.B., Leslie, A.G.W., McCoy, A., et al. (2011). Overview of the CCP4 suite and current developments. Acta Crystallogr. D Biol. Crystallogr. *67*, 235–242. https://doi.org/10.1107/S0907444910045749.

63. Emsley, P., Lohkamp, B., Scott, W.G., and Cowtan, K. (2010). Features and development of Coot. Acta Crystallogr. D Biol. Crystallogr. *66*, 486–501. https://doi.org/10.1107/S0907444910007493.

64. Adams, P.D., Afonine, P.V., Bunkóczi, G., Chen, V.B., Davis, I.W., Echols, N., Headd, J.J., Hung, L.W., Kapral, G.J., Grosse-Kunstleve, R.W., et al. (2010). PHENIX: a comprehensive Python-based system for macromolecular structure solution. Acta Crystallogr. D Biol. Crystallogr. *66*, 213–221. https://doi.org/10.1107/S0907444909052925.

65. Chen, V.B., Arendall, W.B., Headd, J.J., Keedy, D.A., Immormino, R.M., Kapral, G.J., Murray, L.W., Richardson, J.S., and Richardson, D.C. (2010). MolProbity: all-atom structure validation for macromolecular crystallography. Acta Crystallogr. D Biol. Crystallogr. *66*, 12–21. https://doi.org/10.1107/S0907444909042073.

Please cite this article in press as: Arimori et al., Locally misfolded HER2 expressed on cancer cells is a promising target for development of cancer-specific antibodies, Structure (2024), https://doi.org/10.1016/j.str.2024.02.007

CellPress

STAR★METHODS

KEY RESOURCES TABLE

REAGENT or RESOURCE	SOURCE	IDENTIFIER
Antibodies		
Alexa Fluor 488-conjugated anti-mouse IgG	Cell Signaling Technology	Cat#4408; RRID: AB_10694704
FITC-conjugated anti-human IgG	Sigma-Aldrich	Cat#F9512: RRID: AB_259808
Goat Anti-Human Immunoglobulins/HRP	Sigma-Aldrich	Cat#A0170: RRID: AB_257868
Rabbit Anti-Mouse Immunoglobulins/HRP	Dako	Cat#P0260: RRID: AB_2636929
NZ-1	Kato et al.[56]	N/A
H_2Mab-119	Yamada et al.[38]	N/A
H_2Mab-19	Takei et al.[44]	N/A
H_2Mab-41	Kato et al.[46]	N/A
H_2Mab-181	Asano et al.[45]	N/A
Chemicals, peptides, and recombinant proteins		
rProtein A Sepharose Fast Flow	Cytiva	Cat#GE17-1279-01
Capto L	Cytiva	Cat#17547806
Protein G Sepharose 4 Fast Flow	Cytiva	Cat#GE17-0618-01
Ni-NTA Agarose	QIAGEN	Cat#30210
SuperBlock Blocking Buffer	ThermoFisher scientific	Cat#37515
ELISA POD Substrate TMB Kit	Nacalai Tesque	Cat#05298-80
eBioscience Calcein AM Viability Dye	ThermoFisher scientific	Cat#65-0853-39
Lipofectamine LTX	ThermoFisher scientific	Cat#15338100
X-tremeGENE HP DNA Transfection Reagent	Merck KGaA	Cat#6366244001
Deposited data		
H_2Mab-214 Fv-clasp/epitope peptide complex structure	This paper	PDB ID: 8jyq
H_2Mab-119 Fab/HER2 domain I complex structure	This paper	PDB ID: 8jyr
Experimental models: Cell lines		
ExpiCHO-S cells	ThermoFisher scientific	Cat#A29127
Expi293F cells	ThermoFisher scientific	Cat#A14527
Expi293F GnTI- cells	ThermoFisher scientific	Cat#A39240
HEK293T	ATCC	CRL-3216
CHO-K1	ATCC	CCL-61
BT-474	ATCC	HTB-20
SK-BR-3	ATCC	HTB-30
MDA-MB-468	ATCC	HTB-132
MCF 10A	ATCC	CRL-10317
HaCaT	CLS Cell Lines Service GmbH	Cat#300493-ACADEMIC
Experimental models: Organisms/strains		
Mouse: BALB/c Nude	Charles River Laboratories	Strain Code: 194
Recombinant DNA		
pcDNA3.1 vector	ThermoFisher scientific	Cat#V79020
pCAG-Neo vector	FUJIFILM Wako Pure Chemical Corporation	Cat#163-25601
pCAG-Ble vector	FUJIFILM Wako Pure Chemical Corporation	Cat#164-25631
Software and algorithms		
GraphPad PRISM 6	GraphPad Software	https://www.graphpad.com/
GraphPad PRISM 8	GraphPad Software	https://www.graphpad.com/

(*Continued on next page*)

Continued

REAGENT or RESOURCE	SOURCE	IDENTIFIER
FlowJo ver.10	BD Biosciences	https://www.bdbiosciences.com/en-us/products/software/flowjo-v10-software
XDS	Kabsch[60]	https://xds.mr.mpg.de/
PHASER	McCoy et al.[61]	http://www.ccp4.ac.uk
PHENIX	Adams et al.[64]	https://phenix-online.org/
Coot	Emsley et al.[63]	https://www2.mrc-lmb.cam.ac.uk/personal/pemsley/coot/
MOLPROBITY	Chen et al.[65]	http://molprobity.biochem.duke.edu/
PyMOL	Schrödinger, LLC	https://pymol.org/2/

RESOURCE AVAILABILITY

Lead contact

Further information and requests for resources and reagents should be directed to and will be fulfilled by the lead contact, Takao Arimori (arimori@protein.osaka-u.ac.jp).

Materials availability

H_2Mab-214 is available from Tohoku University Graduate School of Medicine.

Data and code availability

Coordinates for the structural models of H_2Mab-214 Fv-clasp/epitope peptide complex and H_2Mab-119 Fab/HER2 domain I complex have been deposited to the Protein Data Bank under PDB accession numbers 8jyq and 8jyr, respectively. All deposited data is publicly available as of the date of publication. This paper does not report original code. Any additional information required to re-analyze the data reported in this paper is available from the lead contact upon request.

EXPERIMENTAL MODEL AND STUDY PARTICIPANT DETAILS

Cell lines

Chinese hamster ovary (CHO)-K1, BT-474, SK-BR-3, MDA-MB-468, HEK293T, and MCF 10A cell lines were obtained from the American Type Culture Collection (ATCC). HaCaT cell line was obtained from Cell Lines Service GmbH (Eppelheim). CHO/HER2 were generated by transfecting pCAG/PA-HER2-RAP-MAP into CHO-K1 cells using Lipofectamine LTX (Thermo Fisher Scientific, Inc.). A few days after transfection, PA tag-positive cells were sorted by a cell sorter (SH800; Sony Corp.) using NZ-1, which was originally developed as an anti-human PDPN mAb.[56]

CHO-K1 and CHO/HER2 were cultured in RPMI-1640 medium (Nacalai Tesque, Inc.) or in Ham's F-12 medium (FUJIFILM Wako Pure Chemical Corporation), and BT-474, SK-BR-3, MDA-MB-468, HEK293T, and HaCaT were cultured in DMEM medium (Nacalai Tesque, Inc.), supplemented with 10% heat-inactivated fetal bovine serum (FBS; Thermo Fisher Scientific Inc.), 100 units/ml of penicillin, 100 μg/ml streptomycin, and 0.25 μg/ml amphotericin B (Nacalai Tesque, Inc.). MCF 10A was cultured in Mammary Epithelial Cell Basal Medium BulletKit™ (CC-3150, Lonza) supplemented with 100 ng/ml cholera toxin (Sigma-Aldrich). All of the above cell lines were cultured at 37°C in a humidified atmosphere with 5% CO_2.

ExpiCHO-S, Expi293F, and Expi293F GnT1- cell lines were obtained from Thermo Fisher Scientific. ExpiCHO-S cells were cultured in ExpiCHO expression medium (Thermo Fisher Scientific), and Expi293F and Expi293F GnT1- cells were cultured in Expi293 expression medium (Thermo Fisher Scientific). Those cell lines were cultured in a shaker at 37°C shaker in a humidified atmosphere with 8% CO_2.

Animals

The animal experiment for generation of anti-HER2 mAbs was approved by the Animal Care and Use Committee of Tohoku University (Permit number: 2019NiA-001). Animal experiments for ADCC and antitumor activity were approved by the Institutional Committee for Experiments of the Institute of Microbial Chemistry (approval no. 2023-001 and 2023-018). BALB/c nude mice were obtained from Charles River Laboratories and maintained and monitored as described previously.[57] The loss of original body weight was determined to a point >25% and/or a maximum tumor size >3,000 mm^3 as humane endpoints for euthanasia.

Please cite this article in press as: Arimori et al., Locally misfolded HER2 expressed on cancer cells is a promising target for development of cancer-specific antibodies, Structure (2024), https://doi.org/10.1016/j.str.2024.02.007

METHOD DETAILS

Antibodies

Anti-HER2 mAb, H_2Mab-119 (mouse IgG_1, kappa), was established as previously described.[38] H_2Mab-214 (mouse IgG_1, kappa) was established by the same strategy. In brief, BALB/c mice were immunized with recombinant HER2-extracellular domain produced by LN229 cells together with Imject Alum (Thermo Fisher Scientific, Inc.). After several additional immunizations, spleen cells were fused with P3U1 cells. The culture supernatants of hybridomas were screened using enzyme-linked immunosorbent assay with recombinant HER2-extracellular domain and flow cytometry. We finally established 278 clones of hybridoma and further performed the screening of reactivity to HER2-positive breast cancers (BT-474 and SK-BR-3) and non-transformed normal epithelial cells including HaCaT and MCF 10A using flow cytometry.

To identify V_H/V_L sequences, total RNA was prepared from the hybridoma cells using an RNeasy PLUS Mini Kit (Qiagen). The initial cDNA strand was synthesized using the SuperScript IV Reverse Transcriptase (Thermo) via a priming oligo-dT, according to the manufacturer's instructions. PCR amplification was performed with oligonucleotide mixtures of the degenerate primer and the constant region primer for the heavy (γ) and light (κ) chains.[58] PCR reactions were performed with HotStar *Taq* polymerase (Qiagen). The PCR products were purified, subcloned into the pCR4-TOPO vector (Thermo), and subjected to nucleotide sequencing.

Variable (V_H) and constant (C_H) regions of heavy chain cDNAs of H_2Mab-119 and H_2Mab-214 were subcloned into the pCAG-Neo vector (FUJIFILM Wako Pure Chemical Corporation). Variable (V_L) and constant (C_L) regions of light chain cDNAs of H_2Mab-119 and H_2Mab-214 were subcloned into the pCAG-Ble vector (FUJIFILM Wako Pure Chemical Corporation). To produce recombinant H_2Mab-119 and H_2Mab-214, the vectors of heavy and light chains were transfected into ExpiCHO-S cells using the ExpiCHO Expression System (Thermo Fisher Scientific Inc.). H_2Mab-119 and H_2Mab-214 were purified using Ab-Capcher (ProteNova Co., Ltd.). Bound antibodies were eluted with an IgG elution buffer (Thermo Fisher Scientific Inc.), followed by immediate neutralization of eluates, using 1M Tris-HCl (pH 8.0). Finally, eluates were concentrated, after which 10 mM sodium phosphate buffer, pH 7.5, 150 mM NaCl (PBS) was used to replace with the elution buffer using Amicon Ultra (Merck KGaA).

To generate H_2Mab-119-mG_{2a}-f and H_2Mab-214-mG_{2a}-f, we subcloned these V_H cDNA and C_H of mouse IgG_{2a} into the pCAG-Ble vector. These V_L cDNA and C_L cDNA of mouse kappa light chain were also subcloned into the pCAG-Neo vector. The vectors for the H_2Mab-119-mG_{2a} or H_2Mab-214-mG_{2a} were transduced into BINDS-09 (FUT8-knockout ExpiCHO-S) cells, and recombinant mAbs were produced using the ExpiCHO Expression System. H_2Mab-119-mG_{2a}-f and H_2Mab-214-mG_{2a}-f were purified using Ab-Capcher. Preparation of 281-mG_{2a}-f (defucosylated anti-hamster PDPN mAb, control defucosylated mouse IgG_{2a}) was previously described.[59] Trastuzumab (Herceptin) was obtained from Chugai Pharmaceutical Co., Ltd (Tokyo, Japan).

Flow cytometry

CHO-K1, CHO/HER2, BT-474, SK-BR-3, MDA-MB-468, HEK293T, HaCaT, and MCF 10A cells were obtained using 0.25% trypsin and 1 mM ethylenediamine tetraacetic acid (EDTA; Nacalai Tesque, Inc.). The cells were treated with primary mAbs (H_2Mab-119, H_2Mab-214, H_2Mab-119-mG_{2a}-f, H_2Mab-214-mG_{2a}-f, or trastuzumab) or blocking buffer (control; 0.1% BSA in PBS) for 30 min at 4°C. Then, the cells were treated with Alexa Fluor 488-conjugated anti-mouse IgG (1:1,000; Cell Signaling Technology, Inc.) or FITC-conjugated anti-human IgG (1:1,000; Sigma-Aldrich for trastuzumab) for 30 min at 4°C.

To analyze the antibody binding to DTT-treated cells, HEK293T, SK-BR-3, and MCF 10A cells were cultured in the media containing 1 mM DTT for 1, 5, 24 hours. The cells were then washed repeatedly with PBS to remove DTT and treated with 0.5 μg/ml of trastuzumab or 10 μg/ml of H_2Mab-119 (mouse IgG_1, kappa), H_2Mab-214 (mouse IgG_1, kappa), H_2Mab-19 (mouse IgG_{2b}, kappa), H_2Mab-181 (mouse IgG_1, kappa), or H_2Mab-41 (mouse IgG_{2b}, kappa) for 1 hour on ice, followed by treatment with 5 μg/ml of Alexa Fluor 488-conjugated anti-human IgG or anti-mouse IgG for 45 min on ice.

For the assessment of antibody binding to HER2 mutants, CHO-K1 cells were transiently transfected with vectors encoding various HER2 mutants or empty vector using X-tremeGENE HP DNA Transfection Reagent (Merck KGaA). The cells were stained with antibodies using the same procedure as for the DTT-treated cells.

All fluorescence data were collected using SA3800 Cell Analyzer (Sony Corp.) and analyzed using FlowJo (BD Biosciences).

Enzyme-linked immunosorbent assay (ELISA)

For the epitope mapping, NUNC Maxisorp 96-well plates (Thermo Fisher Scientific, Inc.) were coated with synthetic peptides (10 μg/ml; PepScreen by Sigma-Aldrich) or HER2ec (10 μg/ml) for 30 min at 37°C and blocked with Superblock reagent (Thermo Fisher Scientific, Inc.) or 1% bovine serum albumin (Nacalai Tesque, Inc.) in 0.05% Tween 20 containing PBS (1% BSA/PBST) for 30 min at 37°C. H_2Mab-214 (10 μg/ml) was then added to the plate and incubated for 30 min at 37°C. To detect bound antibodies, horseradish peroxidase (HRP)-conjugated rabbit anti-mouse IgG antibody (Agilent Technologies) diluted to 1:2,000 in 1% BSA/PBST was added and incubated for 30 min at 37°C. We used ELISA POD Substrate TMB Kit (Nacalai Tesque, Inc.) for the enzymatic reactions. The optical density was measured at 655 nm using an iMark microplate reader (Bio-Rad Laboratories, Inc.).

To determine the binding affinity of trastuzumab, H_2Mab-119, and H_2Mab-214 for HER2, NUNC Maxisorp 96-well plates (Thermo Fisher Scientific, Inc.) were coated with HER2ec (1 μg/ml) for 30 min at 37°C and blocked with 1% BSA/PBST for 1 hour at 37°C. Serially diluted antibody solutions (0.003 to 50 μg/mL, which is approximately 0.04 to 650 nM) were then added to the plate and incubated for 1 hour at 37°C. Detection of bound antibodies was performed as above using HRP-conjugated goat anti-human IgG antibody (Sigma-Aldrich, for trastuzumab) or HRP-conjugated rabbit anti-mouse IgG antibody diluted to 1:3,000 in 1% BSA/PBST. Using

the values of OD_{655} at 25 min after initiating the enzyme reaction, K_D values were calculated by fitting the binding isotherms using *the built-in one-site binding models* in GraphPad PRISM 6 (GraphPad Software, Inc., La Jolla, CA).

ADCC

Spleens were aseptically removed from six female BALB/c nude mice (five-week-old, Charles River Laboratories, Inc.) Single-cell suspensions were obtained using a cell strainer (352360, BD Biosciences). Erythrocytes were removed with the treatment of ice-cold distilled water. The splenocytes were used as effector cells.

H_2Mab-119-mG_{2a}-f and H_2Mab-214-mG_{2a}-f-mediated ADCC was assayed as follows. Target cells (BT-474 and MDA-MB-468) were labeled with 10 μg/ml Calcein AM (Thermo Fisher Scientific, Inc.). The target cells (2×10^4 cells) were plated in 96-well plates (3860-096, AGC TECHNO GLASS Co.,Ltd.) and mixed with effector cells (effector/target cells ratio, 50), 100 μg/ml of H_2Mab-119-mG_{2a}-f, H_2Mab-214-mG_{2a}-f, 281-mG_{2a}-f (control defucosylated mouse IgG_{2a}) or control mouse IgG_{2a} (Sigma-Aldrich). Following incubation for 4.5 h at 37°C, the Calcein release into the medium was analyzed using a microplate reader (Power Scan HT; BioTek Instruments, Inc.,) with an excitation wavelength (485 nm) and an emission wavelength (538 nm).

Cytotoxicity (% lysis) was calculated as follows: % lysis = (E - S)/(M - S) x 100, where "E" is the fluorescence in cultures of both effector and target cells, "S" is the spontaneous fluorescence of only target cells, and "M" is the maximum fluorescence following the treatment with a lysis buffer (10 mM Tris-HCl [pH 7.4], 10 mM EDTA, and 0.5% Triton X-100).

CDC

The Calcein AM- labeled target cells (BT-474 and MDA-MB-468, 2×10^4 cells) were plated in 96-well plates (3860-096, AGC TECHNO GLASS Co.,Ltd.) and mixed with rabbit complement (final dilution 1:10, Low-Tox-M Rabbit Complement; Cedarlane Laboratories) and 100 μg/ml of H_2Mab-119-mG_{2a}-f, H_2Mab-214-mG_{2a}-f, 281-mG_{2a}-f or control mouse IgG_{2a}. Following incubation for 4.5 h at 37°C, Calcein release into the medium was measured as indicated above.

Antitumor activity of H_2Mab-119-mG2a-f and H_2Mab-214-mG_{2a}-f in xenografts of BT-474 and MDA-MB-468 cells

BT-474 and MDA-MB-468 (5×10^6 cells) resuspended in DMEM and mixed with BD Matrigel Matrix Growth Factor Reduced (BD Biosciences) were subcutaneously injected into the left flank of BALB/c nude mice (Charles River Laboratories, Inc). On day 7 post-inoculation, H_2Mab-119-mG_{2a}-f (n=8), H_2Mab-214-mG_{2a}-f (n=8), 281-mG_{2a}-f (n=8) or control mouse IgG (FUJIFILM Wako Pure Chemical Corporation) (n=8) in PBS were intraperitoneally injected (5 mg/kg). On days 14 and 19, additional antibody injections were performed. The tumor volume was measured on days 7, 12, 14, 19, 22, and 26 after the inoculation of cells. Tumor volumes were determined as previously described.[57]

Crystallization

To generate H_2Mab-214 Fv-clasp, V_H (residues 1-113) and V_L (residues 1-108) regions of H_2Mab-214 were appended to SARAH domain derived from human Mst1.[42] Hinge-less Fc (residues 234-447 of human IgG_1) was subsequently appended to the V_L-SARAH. The DNA fragments were subcloned into the pcDNA3.1 vector (Thermo Fisher Scientific, Inc.). V_H-SARAH and V_L-SARAH-Fc were co-expressed in Expi293F cells (Thermo Fisher Scientific, Inc.) and purified with rProtein A Sepharose Fast Flow (Cytiva). The Fc portion was digested by treatment with a His-tagged IdeS protease for 2 hours at 37°C, followed by removal of His-IdeS by Ni-NTA Agarose (QIAGEN). The sample was further purified by anion-exchange chromatography on a MonoQ 5/50 GL column (Cytiva) equilibrated with 20 mM Tris, pH 8.0, and the resultant sample was concentrated by ultrafiltration using Amicon Ultra (Merck Millipore) and mixed with synthetic epitope peptide (residues 611-618 of HER2, MPIWKFPD) to be the final concentration of 5 mg/ml H_2Mab-214 Fv-clasp and 0.6 mM peptide. To prepare the recombinant H_2Mab-119 Fab, the V_H to C_H1 region of the H_2Mab-119 heavy chain was subcloned into the pCAG-Neo vector and co-expressed with the H_2Mab-119 light chain in ExpiCHO-S cells. H_2Mab-119 Fab was purified with Capto L (Cytiva) followed by Protein G Sepharose 4 Fast Flow (Cytiva).

The HER2 domain I (residues 1-216) with a C-terminal His-tag was subcloned into pcDNA3.4 (Thermo Fisher Scientific, Inc.) and expressed in Expi293F GnT1- cells (Thermo Fisher Scientific, Inc.), followed by purification with Ni-NTA Agarose. For the crystallization, H_2Mab-119 Fab was mixed with HER2 domain I at 1.5-fold molar excess and subjected to size-exclusion chromatography (SEC) on a Superdex 200 Increase 10/300 GL column equilibrated with 20 mM Tris, 150 mM NaCl, pH 8.0 (Figure S3C). The purified sample was concentrated to 5 mg/ml by ultrafiltration using Amicon ultra (Merck Millipore).

Crystallization screening was carried out using The Classic Suite (QIAGEN), Wizard Classic 1 & 2 (Rigaku), JCSG-plus (Molecular Dimensions), and ProPlex (Molecular Dimensions) crystallization reagents by using the sitting-drop vapor diffusion method at 20°C.

Data collection, structure determination, and refinement

Crystals of the H_2Mab-214 Fv-clasp/epitope peptide complex obtained under the condition of 0.1 M CHES pH 9.5, 20 % w/v polyethylene glycol (PEG) 8000 (JCSG plus, tube 1-7) and the H_2Mab-119 Fab/HER2 domain I complex obtained under the condition of 0.1M Sodium citrate pH5.5, 20% w/v PEG3000 (JCSG plus, tube 1-2) were cryo-protected by well solution containing 15% PEG200 and 30% PEG3000, respectively.

Diffraction data were collected at 100 K at beamline BL44XU of SPring-8 (Harima, Japan). The data were processed and scaled using X-ray Detector Software.[60] Initial phases were determined by molecular replacement with PHASER[61] in the CCP4 package[62] using the crystal structures deposited in Protein Data Bank (PDB: 7cea for H_2Mab-214 V_H, 7bsc for H_2Mab-214 V_L, 7cea for SARAH

domain, 1f3d for H_2Mab-119 V_H-C_H1, 3wkm for H_2Mab-119 V_L-C_L, and 4hrl for HER2 domain I) as search models. The structural models were modified with COOT,[63] refined with PHENIX,[64] and validated with MolProbity.[65] Data collection statistics and refinement parameters are summarized in Table S1.

QUANTIFICATION AND STATISTICAL ANALYSIS

All data are expressed as mean ± standard error of the mean (SEM). Welch's t test was used for the statistical analyses in ADCC, CDC, and tumor weight. ANOVA with Tukey's post hoc test was used for the statistical analyses in tumor volume and mouse weight. GraphPad Prism 8 (GraphPad Software, Inc.) was utilized for the calculations. $P<0.05$ was considered to indicate a statistically significant difference.